A

DISSERTATION REPORT

ON

STUDY OF PRECIPITATION HARDENING AND DYNAMIC RECRYSTALLIZATION BEHAVIOUR OF COPPER AND TUNGSTEN ADDED 2205 DUPLEX STAINLESS STEELS

By

NEERAJ KUMAR
(2015PSL5309)

UNDER THE SUPERVISION OF
Prof. Malay Kumar Banerjee
Department of Metallurgical and Materials Engineering

Submitted in partial fulfillment of the requirement of the degree of

MASTER OF TECHNOLOGY
IN
STEEL TECHNOLOGY

DEPARTMENT OF METALLURGICAL AND MATERIALS ENGINEERING
MALAVIYA NATIONAL INSTITUTE OF TECHNOLOGY JAIPUR
JAIPUR-302017 (RAJASTHAN) INDIA
JUNE-2017

MALAVIYA NATIONAL INSTITUTE OF TECHNOLOGY

DEPARTMENT OF METALLURGICAL & MATERIALS ENGINEERING
JAIPUR-302017 (RAJASTHAN) INDIA

CERTIFICATE

*This is to certify that the project report entitled "**Study of Precipitation Hardening and Dynamic Recrystallization behaviour of Copper and Tungsten added 2205 Duplex Stainless Steels",** submitted by **Neeraj Kumar (College ID: 2015PSL5309)** towards the partial fulfilment of the requirement for the degree of **Master of Technology (M.Tech.)** in the field of **Steel Technology** of **Malaviya National Institute of Technology, Jaipur** is a record of the confide work carried out by him under my supervision. The work submitted, in my opinion, has reached to a level required for being accepted for the examination.*

The matters embodied in this project work, to the best of my knowledge, have not been submitted to any other University or institute for the award of any degree or diploma.

.....

Place: MNIT, Jaipur

Date: June 2017

Prof. MALAY KUMAR BANERJEE

Metallurgical & Materials Engg. Deptt.

MNIT, Jaipur

MALAVIYA NATIONAL INSTITUTE OF TECHNOLOGY

DEPARTMENT OF METALLURGICAL & MATERIALS ENGINEERING
JAIPUR-302017 (RAJASTHAN) INDIA

DECLARATION

*I hereby declare that the dissertation entitled "**Study of Precipitation Hardening and Dynamic Recrystallization behaviour of Copper and Tungsten added 2205 Duplex Stainless Steels",** being submitted by me towards the partial fulfilment of the requirement for the degree of **Master of Technology (M.Tech.)** in the field of **Steel Technology** of **Malaviya National Institute of Technology, Jaipur** is a research work carried out by me is an authentic record of my own under the supervision of Prof. Malay Kumar Banerjee, Department of Metallurgical & Materials Engineering, Malaviya Institute of Technology, Jaipur.*

.....

Place: MNIT, Jaipur

Date: June 2017

Mr. NEERAJ KUMAR

Metallurgical & Materials Engg. Deptt.

MNIT, Jaipur

ACKNOWLEDGEMENT

I would like to convey my heartiest thanks and gratitude to my supervisor **Prof. Malay Kumar Banerjee**, Ministry of Steel Chair Professor at Department of Metallurgical and Materials Engineering, Malaviya National Institute of Technology Jaipur, for providing me this great opportunity to work under him and for his constant guidance and encouragement throughout the dissertation work.

I want to thank **Prof. A. K. Bhargava**, Head of the Department, Metallurgical and Materials Engineering, MNIT Jaipur for giving me permission to commence this dissertation in the first instance, to do necessary research work even after the working hours of the department and to use different equipments and machines. I sincerely extend my deep gratitude to **Dr. R. K. Duchaniya**, Convener, DPGC, Department of Metallurgical and Materials Engineering, MNIT Jaipur for his encouragement and necessary permissions to carry out the work.

I would like to express my sincere gratitude to **Mr. Mukesh Kumar Chowrasia** , **Mr. Arun Kumar** and **Mr. Akshay Kumar,** Research Scholars at MNIT Jaipur for helping me throughout my dissertation work.

I sincerely acknowledge the support rendered by **Shri Lalaram ji, Shri Lalchand ji, Shri Nathuram ji** for helping me during my work. I would also like to thank **Mr. Bhupesh, Mr. Jai, Ms. Arti** from Materials Research Centre(MRC) for helping me during characterization.

I would also like to thank **Mr. Rajendra Shamra, Mr. Mrinmoy Sinha ,Mr. Sumit, Mr. Prabha Joyti Patra** for helping me out during Thermo-mechanical simulation(Gleeble) at IIT Roorkee.

I would specially like to thank my friends **Ms. Bhawna Jarwal, Mr. Deepak Kumar, Mr. Md. Asgar Ali, Mr. Mayank Sunariwal** for their enormous help and support in conducting this work.

I am truly thankful to my beloved parents for their wishes, encouragement, continuous support and motivation in conducting the work successfully.

Last, but not the least, I am also thankful to all known and unknown persons who helped me directly or indirectly during my dissertation work.

I am sure that this dissertation would have not been possible without their support, understanding and encouragement.

NEERAJ KUMAR
M.Tech(Steel Technology)

ABSTRACT

Duplex stainless steels are having 50-50 ferrite and austenite structure. The designing of Duplex stainless steels is an art as it contains Cr and Ni in a proportion to maintain the ratio of its phases. This is possible because chromium is a ferrite stabilizer whereas nickel is a austenite stabilizer. The 2205 grade of DSS contains 22%Cr and 5%Ni and also 2.5-3%Mo. These alloying elements are of prime importance as precipitation hardening because of the feasibility of formation of precipitates at higher temperatures. There are various intermetallic phases that precipitate along these grains and grain boundaries. These phases are responsible for increasing the hardness values of duplex stainless steels. These intermetallic phases increase the hardness properties of these steels by compromising with its other mechanical and as well as with its corrosion resistivity property.

As these intermetallic phases are detrimental for properties of duplex stainless steels and hence, the current study focuses on addition of Copper(Cu) and Tungsten(W) as both are responsible in decreasing the rate of formation of these precipitates and instead form copper precipitates for its hardening through precipitation of copper. Copper and tungsten not only form their own precipitates at different temperatures but also decrease the rate of formation of detrimental sigma and chi phases.

Casting was done in induction furnace of DSS to alloy copper and tungsten followed by forging and rolling. DSC, XRD, Hardness, SEM analysis were done by varying ageing temperature and ageing time. The studies have shown partial precipitation of copper at ageing temperatures of around 300°C and precipitation of tungsten at 850°C.

Thermo mechanical treatment was performed on Gleeble 3800 by hot compression test by varying temperature and strain rate to study Dynamic recrystallization behaviour(DRX). Generally dynamic recrystallization behaviour occurs at low strain rates but in our study we have seen this at strain rate 1 and 10 also at 1100°C. Serrated curves were observed at strain rate 1 with varying temperatures at 900°C, 1000°C and 1100°C. These serrations are due to Dynamic strain ageing. At high strain rate i.e. at 20 no Dynamic recrystallization is observed. Dynamic recovery(DRV) and strain hardening is also observed in other cases.

Based on this study it is concluded that precipitation hardening could be done in duplex stainless steels through copper and tungsten addition. Thermo mechanical treatment showed Dynamic recrystallization at low strain rates but at high strain rates dynamic recrystallization behaviour was affected as the Dynamic strain ageing and strain hardening factors were more dominant.

The entire work has been presented over seven chapters in the dissertation. **Chapter 1** presents the introduction of the work. A review of literature survey is presented in **Chapter 2** which describes the types of Stainless steels, their properties and applications. It also deals with the fact that why duplex stainless steel was selected as a choice for this project. It also deals with the fact that why only copper and tungsten were added to 2205 grade of duplex stainless steel. **Chapter 3** deals with the formulation of the problem and gaps found in literature and research question. **Chapter 4** shows the experimental procedure of the work performed. **Chapter 5** formulates Results and discussion for the performed experiments. **Chapter 6** concludes the dissertation. **Chapter 7** Suggestions for future work.

LIST OF CONTENTS

LIST OF FIGURES

LIST OF TABLES

LIST OF ABBREVIATIONS

SS	Stainless steel
DSS	Duplex stainless steel
IGC	Inter-granular corrosion
SCC	Stress corrosion cracking
DBTT	Ductile to brittle transition temperature
AOD	Argon oxygen decarburization
LDX	Lean duplex stainless steel
SDSS	Super duplex stainless steel
HDSS	Hyper duplex stainless steel
PREN	Pitting resistance equivalent number
BSE	Back-scattered electron microscopy
SEM	Scanning electron microscopy
CPT	Critical pitting temperature
IGA	Inter-granular attack
DOS	Degree of sensitization
DRX	Dynamic recrystallization
DRV	Dynamic recovery
DSC	Differential scanning calorimetry
XRD	X-ray diffraction

Chapter 1

Introduction

Stainless steels (SS) are high alloy steels and possess excellent corrosion and oxidation resistance. These steels contain large amounts of Chromium, Nickel with addition to other alloying elements like Molybdenum, Manganese, Titanium, Niobium, Copper, Tungsten, Selenium, Aluminium, Nitrogen and Tantalum. The corrosion resisting property is due to a thin, adherent, stable Chromium oxide or Nickel oxide film that effectively protects the steel against many corroding media. Corrosion property is induced only when the steel contains a minimum of 11.5% Chromium. Due to these characteristics, these steels find numerous applications in marine applications, nuclear plants, power generating units, paper manufacturing plants, food processing units and petroleum industries.

Duplex Stainless Steels (DSS) have an excellent combination of mechanical, corrosion and welding properties and thus suitable for oil, chemical, marine and petrochemical applications, particularly where chlorides are present. There are various grades of Duplex Stainless Steel used for specific applications.

DSS, generally suffer from pitting corrosion, Intergranular corrosion (IGC), Stress corrosion cracking (SCC) during long service conditions due to precipitation of intermetallic phases which not only affect the corrosion properties but also affect the mechanical properties of DSS.

Hence, the project work deals with designing of Duplex Stainless Steel with alloying elements like Copper(Cu) & Tungsten(W) and after dynamic recrystallization, studying the effects on mechanical and corrosion properties and also its behaviour towards precipitation hardening due to various alloying elements.

Duplex stainless steel is a dual phase (austenite and ferrite) stainless steel and the composition is so adjusted that it could get around 50% of both the microstructures. Hence, a duplex grade was taken by me as my research material as it can give many combined advantages of both the phases. 2205 duplex stainless steel is a standard grade when we talk about the family of duplex stainless steel. The dual phase nature of these steel make them innovative from other groups of stainless steels. The basic concept of my project work was just to design a stainless steel with alloying copper and tungsten as the addition of these elements not only decrease the rate of formation of detrimental intermetallic phases but also form their own precipitates at different ageing temperatures which increase the precipitation hardening of these stainless steels. Tungsten also increases PREN value that is also an advantage for our steel.

Study of hot compression behaviour of Cu and W added 2205 duplex stainless steel was performed using Gleeble 3800 simulator at various strain rates and temperatures. The study was performed at strain rates 1, 10, 20 and temperatures 900°C, 1000°C, 1100°C. Stress vs Strian curves were drawn and were analysed. The Dynamic recrystallization behaviour (DRX) was seen 1 and 10 strain rate at 1100°C. Other mechanisms like dynamic recovery (DRV), dynamic strain ageing and strain hardening.

1.1 Outline of workplan

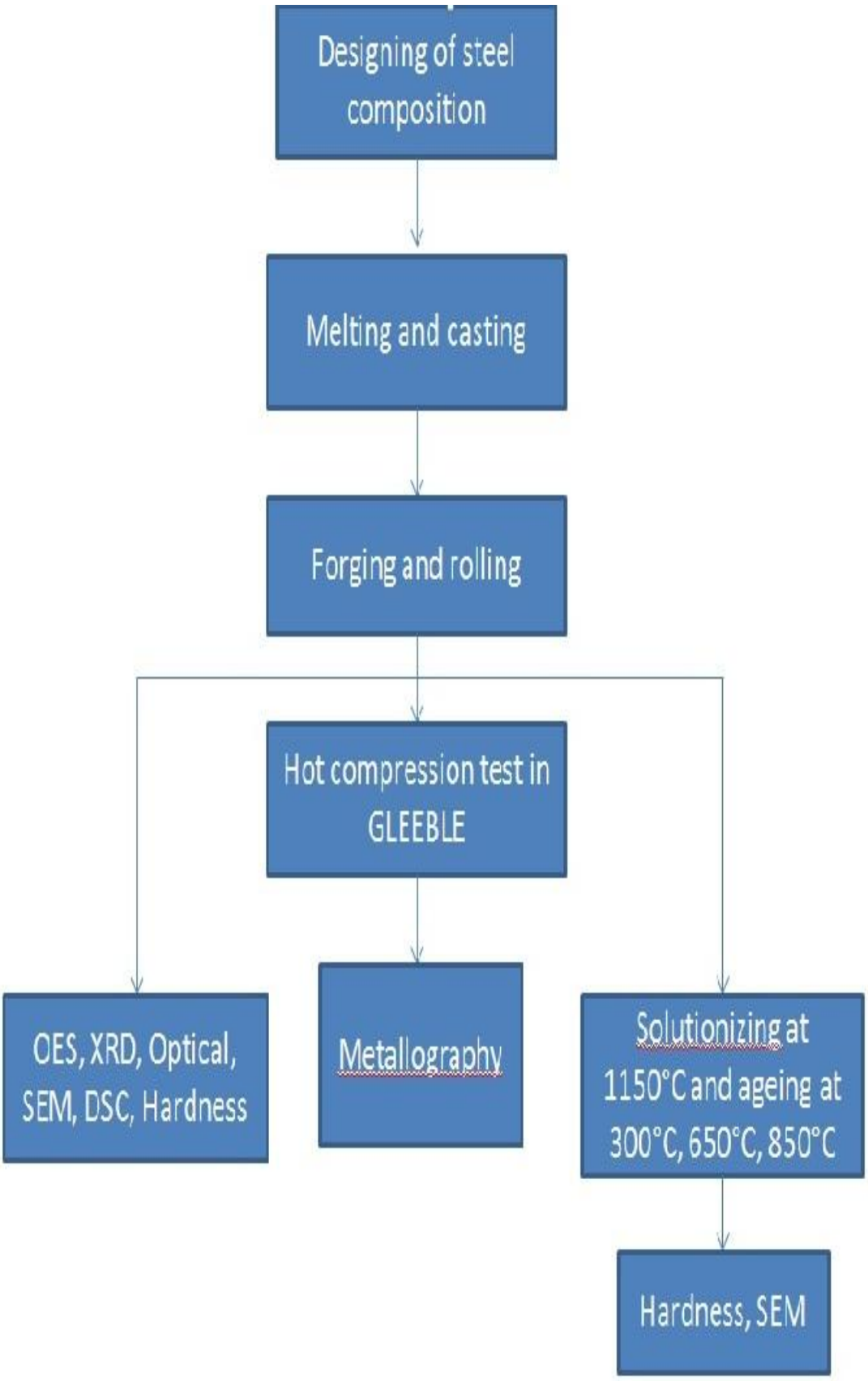

Chapter 2

Literature Review

2.1 Stainless steels

Stainless steels(SS) are iron based high alloy steels or say special purpose steels which do not leave any stain on interacting with corrosive media and hence the name stainless is quoted before these steels. Stainless steels posses excellent corrosion and oxidation resistance as they contain a minimum of 11.5% Chromium(Cr) and this Cr is responsible for introducing corrosion resistance property to these steels. With chromium as the major alloying element other elements are also added to these steels to improve its corrosion as well as mechanical properties. Elements like Nickel(Ni), Molybdenum(Mo), Tungsten(W), Titanium(Ti), Niobium(Nb), Zirconium(Zr), Copper(Cu), Sulphur(S), Manganese(Mn), Silicon(Si), Selenium(Se), Cerium(Ce), Carbon(C) and Nitrogen(N) are added to stainless steels. Elements like Nickel, Molybdenum, Nitrogen also enhance the corrosion resistivity of stainless steels [1,2].

Stainless steels belong to a class of steels which are very flexible i.e., they can be easily designed to exhibit wide range of engineering properties by alloy design and controlled mechanical treatments to meet the demanding conditions. This flexibility has resulted in an improved demand for stainless steels in a broad variety of applications ranging from small pins to a construction of automobiles, petrochemical, aeronautics, ship building industries and nuclear power stations.

Depending on the mechanical properties and composition variations, family of stainless steel is divided into hundreds of grades. The adjustment in the chemical composition and their mechanical treatments play a vital role in improving the corrosion and oxidation resistivity of stainless steel. The large variation in chemical composition leads to formation of different micro-constituents in stainless steels, like Austenitic stainless steels (ASS) have austenitic structure at room temperature when observed through a microscope, similarly Ferritic stainless steels (FSS) contain ferrite structure at room temperature and Duplex stainless steels (DSS) contain dual phases(ferrite and austenite) at room temperatures. Small variation in chemical composition often leads to small change in corrosion and mechanical properties. Example, with slight increase in chemical composition of Austenitic stainless steel (ASS) to improve its corrosion and mechanical properties leads to the formation of Super-Austenitic Stainless steels (SASS) and in case of Duplex stainless steels (DSS) with increase in chemical composition they often form Super-duplex stainless steels (SDSS), Hyper-duplex stainless steels (HDSS) and with decrease in chemical composition Duplex Stainless Steels form Lean-duplex stainless steels(LDX).

The selection for any grade of stainless steel for a particular application depends on following properties:

i. Corrosion(uniform) and oxidation resistance
ii. Resistance to pitting corrosion
iii. Creep strength
iv. High resistance to scaling and oxidation at elevated temperature
v. Strength and hardness
vi. Ductility and formability
vii. Weldability and machinability

viii. Low temperature properties

Stainless steels were discovered and developed at England and Germany in 1910. The commercial production and use of stainless steel took place at United states in 1920s. Initially, it was martensitic stainless steels and ferritic stainless steels (Fe-Cr steels) which were commercially used, but soon the austenitic stainless steels(Fe-Cr-Ni steels) became popular. The use of austenitic stainless steels increased exponentially because the production and fabrication, particularly welding were quite easy when compared with martensitic and ferritic grades.

Most important refining techniques for stainless steels were developed in the 1970s. Argon oxygen decarburization(AOD) and other techniques with different partial gas injections or partial pressure systems allowed the removal of carbon without substantial loss of chromium to the slag. Through these techniques, alloying of other elements also became more easier and also very low levels of sulphur and oxygen could be achieved.

Today, stainless steel has became a potential material for several applications like domestic utensils, fasteners, cutlery, equipments for use in chemical plants, food processing plants, chemical and petrochemical industries, nuclear industries, power plants and transportation industries. Few of the stainless steels are specially manufactured for applications at elevated temperatures or at cryogenic temperatures or at highly corrosive environments.

A set of three-number system is used to identify the stainless steels. The last two digits have no significance, but the first numeral indicates the group as mentioned below:

Series Designation	Group
2××	Cr-Ni-Mn, austenitic, non-magnetic, non hardenable
3××	Cr-Ni, austenitic, non-magnetic, non hardenable
4××	Cr, martensitic, magnetic, hardenable
4××	Cr, ferritic, magnetic, non hardenable
5××	Cr, low chromium, heat resisting

Table 1: Designation of stainless steels[1]

2.2 Types of stainless steels

Stainless steels are divided into five categories. Out of the five categories, four are based on the characteristic crystallographic structure and microstructure of the stainless steels and the fifth, Precipitation hardenable stainless steel(PHSS), is based on heat treatment used than the microstructure.

1.) Martensitic stainless steels
2.) Ferritic stainless steels
3.) Austenitic stainless steels
4.) Duplex stainless steels
5.) Precipitation hardening stainless steels

2.2.1 Martensitic stainless steels

These stainless steels are straight chromium steels containing between 11.5 and 18 percent chromium. These steels are the cheapest among the family of stainless steels. Martensitic stainless steels can be heat treated to improve the mechanical properties. Carbon content of Martensitic stainless steels is one of the important parameters which controls the properties of heat treated steels. They are magnetic in nature, have good toughness, show good corrosion resistance. These steels can be cold worked easily with low carbon content. Martensitic stainless steels can be hardened by oil quenching from austenitizing temperature which depends on the chemical composition of steel.

Composition of Martensitic stainless steels is based on :

$$\%Cr - (17)\%C \leq 12 \qquad \textbf{(1)}$$

Grades 410 and 416 are the most popular alloys in this group and are used for turbine blades and corrosion-resistant castings.

Grade	%C	%Mn	%Si	%Cr	%Ni	%P	%S	others	%Fe
403	0.15	1.00	0.50	11.5-13.0	-	0.04	0.03	-	Bal.
410	0.15	1.00	1.00	11.5-13.5	-	0.04	0.03	-	Bal.
414	0.15	1.00	1.00	11.5-13.5	1.25-2.5	0.04	0.03	-	Bal.
416	0.15	1.25	1.00	12.0-14.0	-	0.06	0.15	0.6Mo	Bal.
416Se	0.15	1.25	1.00	12.0-14.0	-	0.06	0.06	0.15Se	Bal.
420	0.15min.	1.00	1.00	12.0-14.0	-	0.04	0.03	-	Bal.
431	0.20	1.00	1.00	15.0-17.0	1.25-2.5	0.04	0.03	-	Bal.
440A	0.06-0.07	1.00	1.00	16.0-18.0	-	0.04	0.03	0.75Mo	Bal.
440B	0.7-0.9	1.00	1.00	16.0-18.0	-	0.04	0.03	0.75Mo	Bal.
440C	0.9-1.2	1.00	1.00	16.0-18.0	-	0.04	0.03	0.75Mo	Bal.

Table 2: Different grades of Martensitic stainless steels

Martensitic stainless steels find applications as Cutlery items, surgical instruments, high quality ball bearings, valves and high quality knives.

(a)

(b)

Fig. 1: (a) Surgical instruments, (b) High quality knife

2.2.2 Ferritic stainless steels

These steels are similar to martensitic stainless steels as they are also straight chromium steels with 14-27 percent chromium. These steels are superior to martensitic stainless steels in their corrosion resistance but are expensive. These steels cannot be hardened by heat treatment and are moderately hardened by cold working. They are magnetic in nature and can be cold-worked or hot-worked, but they develop their maximum softness, ductility and corrosion resistance in the annealed condition. Since the Ferritic stainless steels may be cold formed easily, they are used extensively for deep-drawn parts such as vessels for chemical and food industries.

Composition of ferritic stainless steels is based on :

$$\%Cr - (17)\%. \ > 12.7 \qquad \textbf{(2)}$$

Grade	%C	%Mn	%Si	%Cr	%Ni	%P	%S	Others	%Fe
405	0.08	1.00	1.00	11.5-14.5	-	0.04	0.03	0.1-0.3Al	Bal.
409	0.08	1.00	1.00	10.5-11.7	0.50	0.04	0.04	0.75max.Ti	Bal.
429	0.12	1.00	1.00	14.0-16.0	-	0.04	003	-	Bal.
430	0.12	1.00	1.00	16.0-18.0	-	0.04	0.03	-	Bal.
430F	0.12	1.25	1.00	16.0-18.0	-	0.06	0.15	0.6Mo	Bal.
442	0.20	1.00	1.00	18.0-23.0	-	0.04	0.03	-	Bal.
446	0.20	1.50	1.00	23.0-27.0	-	0.04	0.03	0.25N	Bal.

Table 3: Different grades of ferritic stainless steels

Ferritic stainless steels are used as kitchen sinks, decorative trim, annealing baskets, nitric acid tanks, dairy machinery, automotive exhaust components stainless nuts and bolts and furnace parts.

(a) **(b)**

Fig. 2: (a) Kitchen sink, (b) Automotive exhaust component

2.2.3 Austenitic stainless steels

These steels are generally Cr-Ni steels with a minimum total chromium and nickel contents of 25 percent. In general, minimum 8 percent nickel and 17 percent chromium contents are essential to make the steel completely austenitic in the presence of low carbon contents. These steels though costly, possess the best possible corrosion properties. 18/8(or 304) is the most widely used grade of Austenitic stainless steel because of their optimum combination of strength, ductility and toughness. These stainless steel grades are non-magnetic in nature. There is no phase transformation with temperature for this class of stainless steels. For this reason, they are not subjected to heat treatment operations in order to improve the properties. Cold working is the only strengthening mechanism for these stainless steels.

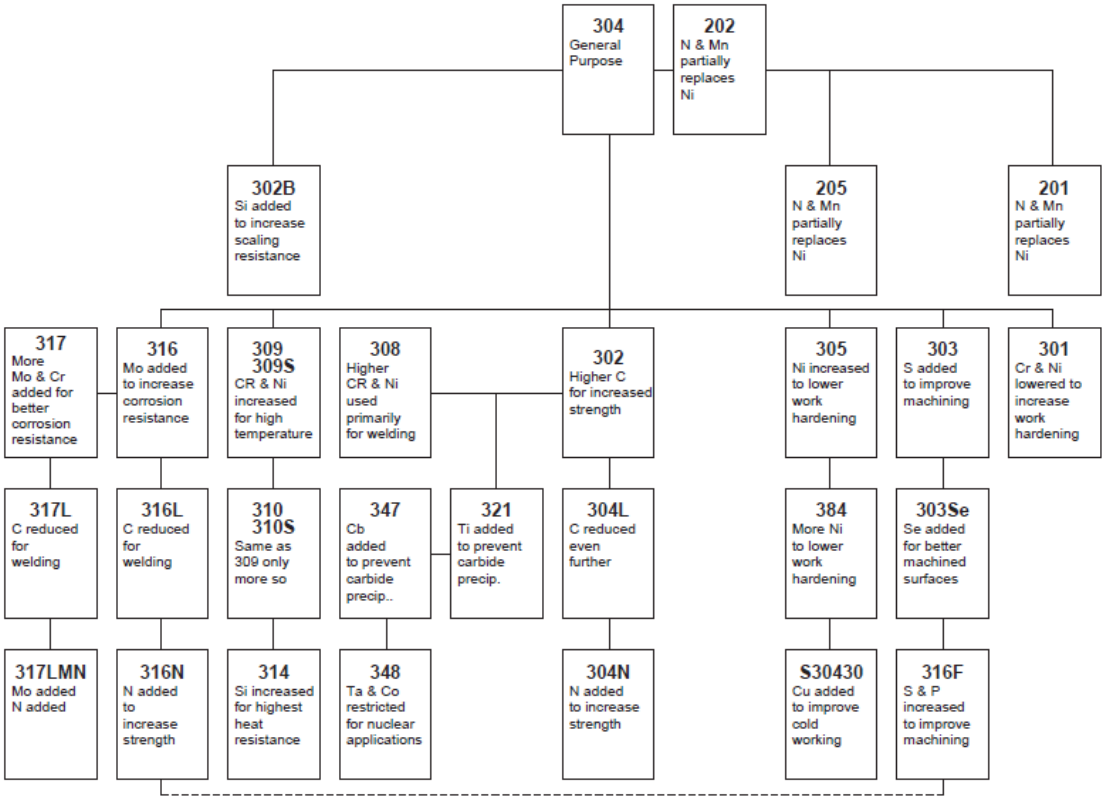

Table 4: Different grades of austenitic stainless steels[1]

Austenitic stainless steels are used as cookware utensils, thermosteel bottles, these steels are also used in cryogenic application as they do not show ductile to brittle transition (DBTT).

Grade 904L was one of the first corrosion resistant grade of austenitic stainless steel developed for petro-chemical industries, which contains 4-5% Mo and 0.2% N. Austenitic stainless steel with higher amount of Molybdenum (6.5%) was developed to improve the resistance to crevice and pitting corrosion in chloride environments. The major drawback for high Mo austenitic stainless steels was that, higher molybdenum content promotes formation of various intermetallic phases at various temperatures.

(a) **(b)**

Fig. 3: (a) Cookware, (b) Cryogenic Tanks

2.2.4 Precipitation hardening stainless steels

These steels have either austenitic or martensitic matrix. Steels with martensitic matrix are more common in the use than austenitic matrix. The austenitic precipitation hardening stainless steels are non-magnetic in nature and have a minimum nickel content of 10 percent. It ensures formation of austenitic matrix which is strengthened by addition of molybdenum, copper, niobium and titanium. Precipitation hardening stainless steels are generally solution annealed at the mill and supplied in that condition. After forming are aged to attain the increase in hardness and strength.

Grade	%C	%Mn	%Si	%Cr	%Ni	%Mo	%Others	%Fe
17-4 PH	0.04	0.40	0.50	16.50	4.25	--	0.25Nb, 3.60Cu	Bal.
17-7 PH	0.07	0.70	0.40	17.00	7.00	--	1.15Al	Bal.
PH 15-7 Mo	0.07	0.70	0.40	15.00	7.00	2.25	1.15Al	Bal.
17-10 P	0.12	0.75	0.50	17.00	10.50	--	0.28P	Bal.

Table 5: Different grades of Precipitation hardening stainless steels[1]

These steels find application in oil field valve parts, aircraft fittings, fasteners, nuclear reactor components, gears, missile fittings and aircraft landing gears.

(a)

(b)

Fig. 4: (a) Aircraft landing gears, (b) Excellent quality fasteners

2.2.5 Duplex stainless steel

The discovery of duplex microstructure in stainless steels was first described by Bain and Griffiths in 1927, but it was not until the 1930s for DSS to be commercially available in the market for its use. Duplex stainless steel(DSS) contains ferrite and austenite phases in their microstructure combined of approximately equal amounts(50-50) by both the phases[3],this is attained by balancing the nickel and chromium contents in DSS.

The development of DSS is divided into two major generations, the first generation of duplex stainless steels were chromium, nickel and molybdenum ferrous alloys where as second generation alloys with the discovery of AOD route were developed by the addition of nitrogen which improved the corrosion resistance and weldability of these alloys. In the early 1980's the discovery of super duplex stainless steels grades increased the application of these stainless steels in highly aggressive offshore and petrochemical industries. This was followed by the discovery of lean duplex grades containing lower alloy contents for applications in less critical sections.

Since 1990s, duplex stainless steels gained a place over austenitic grades of stainless steels because austenitic grades contain large amounts of nickel which is quite costly metal. Metallurgical techniques, improved weldability and greater availability of products have also played a vital role in cementing the importance of duplex stainless steels. Duplex stainless steels are today universally accepted as a reliable solution for corrosion related issues in a number of applications.

Duplex stainless steels have better strength than austenitic or ferritic stainless steels, and excellent resistance to corrosion (comparable to austenitic ones),pitting and crevice corrosion resistivity is also high for certain duplex grades, immunity to stress corrosion cracking(SCC) and good weldability are some salient features of duplex stainless steels. Duplex stainless steels have significantly better ductility than ferritic grades and inferior to austenitic stainless steels but toughness of Duplex stainless steels is better than both ferrtic and austenitic stainless steels. It may often be possible to reduce the section thickness of duplex stainless steels, due to its increased yield strength compared to austenitic grades [4].

DSS exhibit an attractive combination of mechanical properties and corrosion resistance and are thus widely used in various applications such as power plants, desalination facilities, the marine industry, off-shore industries, food industries, chemical industries, paper industries, nuclear industries and in structural industries[5]. Duplex grades, are cost effective because of low nickel and molybdenum content when compared with austenitic counter grades of similar corrosion resistance. They are also more resistant to pitting corrosion, stress corrosion cracking, intergranular corrosion, abrasion and wear.

2205 grade contains nitrogen(0.14-0.20%), it contributes to high temperature stability of the two-phase microstructure particularly in the welded areas. Second, it also improves pitting as well as crevice corrosion resistance properties. Third, nitrogen is also known to reduce intermetallic kinetics [6].

Duplex stainless steels, based on their chemical composition and corrosion resistivity on PREN scale, can be divided into four major groups. These are as follows:

Grades	**Lean DSS**	**Standard DSS**	**Super DSS**	**Hyper DSS**
	S32101	S31803	S32750	S32707
	S32304	S32205	S32520	S33207
	S32404		S32760	

Table 6: Various grades of DSS[6]

Grade	%C	%Mn	%P	%S	%Si	%Cr	%Ni	%Mo	%N	%Fe
S32101	0.03	5.7	0.03	0.02	0.4	21.4	1.2	0.31	0.23	bal.
S32304	0.03	2.50	0.04	0.03	1.00	21.50-24.50	3.0-5.5	0.05-0.6	0.05-0.20	bal.
S31803	0.03	2.00	0.03	0.02	1.00	21-23	4.5-6.5	2.5-3.5	0.08-0.20	bal.
S32205	0.03	2.00	0.03	0.02	1.00	22-23	4.5-6.5	3-3.5	0.14-0.20	bal.
S32750	0.03	1.20	0.03	0.03	1.00	24.0-26.0	6.0-8.0	3.0-3.5	0.24-0.32	bal.
S32760	0.03	1.00, W-0.5-1	0.03	0.01	1.00	24.0-26.0	6.0-8.0	3.0-4.0	0.20-0.30	Cu-0.5-1, bal.

Table 7: Chemical composition of some common DSS grades

2.3 **Schaeffler Diagram**

The schaeffler diagram (Fig. 5) is used to predict the microstructure for stainless steel. Schaeffler divided the alloying elements in two groups: ferrite and austenite stabilizers. Schaeffler developed a formula by means of which the element of each group can be expressed as equivalent chromium content and as equivalent nickel content [7]. The schaeffler diagram evaluate the presence of austenite, ferrite and martensite depending on the chemical composition and the “proper cooling” (or heat treatment) after pouring.

The Schaeffler diagram is very useful during steel making. One can use the chemical composition of the molten steel before pouring to predict the microstructure of the steel. The Schaeffler diagram will indicate whether the material will comply with the required standards or not. The correctness, if required can be made in the composition before pouring and casting.

There are several formulae for the nickel- and chromium-equivalent, each of them giving a somewhat better result for a particular type of stainless steel. In this case we use the formula as indicated here. The most important is that a foundry does use one formula and check the

structure. By doing this they can always evaluate the influence of a fluctuating chemical composition.

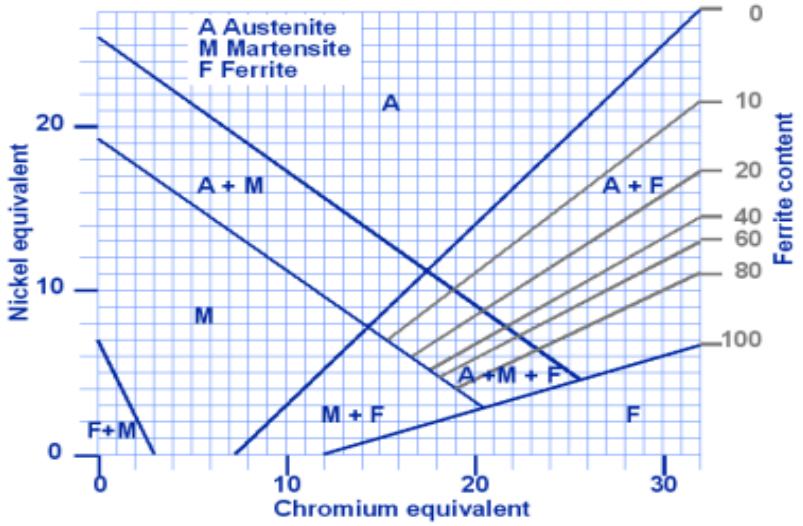

Fig. 5: Schaeffler diagram

The latest version of Chromium and Nickel-equivalent are:

Chromium equivalent = 0.75(%W)+ 1(%Cr)+ 1.5(%Mo+ %Ti)+ 2(Si)+ 5(V)+ 5.5(Al)

Nickel equivalent = 0.3(%Cu)+ 0.5(%Mn)+ 1(%Co+ %Ni)+ 25(N)+ 30(C)

2.3.1 Modified schaeffler diadram

The schaeffler diagram (Fig. 6) was originally developed for welding. Later on it was commonly used to estimate the phases present in stainless steel at room temperature. However the forecast agreement with actual data was markedly reduced where carbide formation took place. In addition, an accurate prediction was complicated either by a lower content (or absence) of Cr and Ni in the weld, or by a higher content of Mn (above 4%). This was attributed to the following factors.

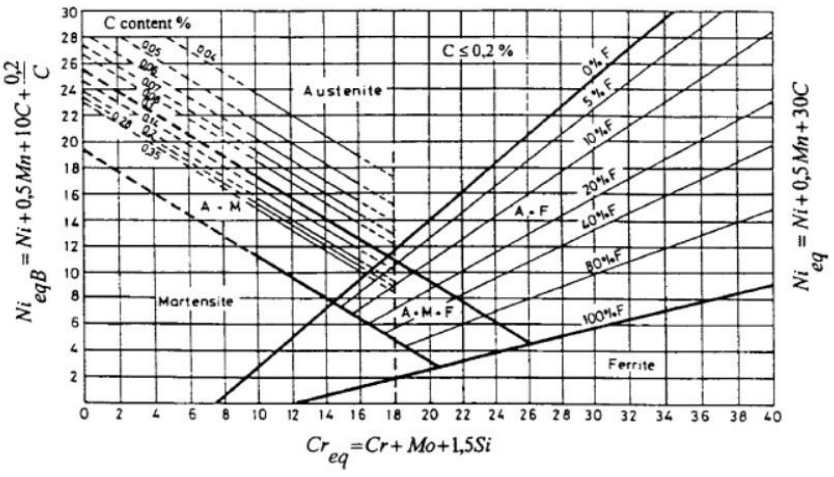

Fig. 6: Modified schaeffler diagram[7]

1. The carbide formation process in weld.
2. Use of constant empiric coefficients in the equation determining Cr and Ni equivalents
3. The difficulty of determining the volume of a specific phase in multiphase zones.

Therefore, the schaeffler diagram was modified to provide a more accurate prediction of weld structure. The coefficients in Cr and Ni equivalents equations were varied depending on the concentration and mutual influence of alloying components, and on the carbide formation process in the weld. The percentage of each phase was decided for interface zone.

2.4 Effect of alloying elements in DSS

The major alloying elements in duplex stainless steels are chromium(Cr), nickel(Ni), molybdenum(Mo) and nitrogen(N).

Chromium:

Chromium is the major alloying element in stainless steel. It is a ferrite stabilizing element i.e. it stabilizes ferrite phase at room temperature. It is the most important alloying element in stainless steel as when chromium content increases from 10.5% it forms a protective oxy-hydroxide layer which is responsible for corrosion resistivity in stainless steels. The strength of the protective layer increases with the increase in chromium content. For addition of nitrogen in DSS it is desirable to have high chromium content. But with increase in chromium content the feasibility for the formation of detrimental intermetallic phases increases in DSS. The chromium equivalent in DSS is given by[5]:

$$Cr_{eq} = \%Cr + (\%Mo) + 0.7(\%Nb)$$

Nickel:

Nickel enhances the corrosion resistance property of stainless steels. Nickel is a austenite stabilising element and minimum 8% nickel is needed to form stable austenite phase at room temperature. Nickel plays a important role in balancing the two phases in duplex stainless steels. Increasing nickel content to more than 8% in austenitic steels improves both corrosion resistivity(in acidic environments) and workability. High nickel content in DSS leads to the formation of alpha-prime phase in ferrite which leads to the embrittlement in the material. Nickel equivalent in DSS is given by[5]:

$$Ni_{eq} = \%Ni + 35(\%C) + 20(\%N) + 0.25(\%Cu)$$

Molybdenum:

It is a ferrite stabilizing element. Molybdenum also increases the resistivity towards general corrosion as well as localized corrosions like pitting and crevice. High amount of Mo results in the resistance of the stainless steels to severe corrosion attacks, example in reducing acids and oxidizing chloride environments. PREN(pitting resistance equivalent number) equation also shows the pitting resistivity property of molybdenum. The pitting property of Mo is 3.3 times more than Cr.

$$PREN_{16} = \%Cr + 3.3(\%Mo + 0.5(\%W)) + 16(\%N)$$

$$PREN_{30} = \%Cr + 3.3(\%Mo + 0.5(\%W)) + 30(\%N)$$

Generally $PREN_{16}$ is used for austenitic stainless steels and $PREN_{30}$ is used for duplex stainless steels [8].

Nitrogen:

Nitrogen is a austenite stabilizing element. It is strong austenite former than nickel and hence helps in stabilizing the dual phases in duplex stainless steels. Nitrogen also enhances strength of DSS by solid solution strengthening. It is also very important element when it comes to resistance to localised corrosion(like pitting and crevice). Nitrogen is known to delay the precipitation of intermetallic phases. But high nitrogen content increases the feasibility of formation of nitrides as precipitates [9].

2.5 Classification of various phases in DSS

The art of duplex stainless steel is the 1:1 ratio of both the ferrite and austenite phases. If somehow this ratio is disturbed, it severely affects its properties. Like in the case of welding, this ratio is disturbed because of the formation of ferrite phase from the austenite grains which is known as ferritization. As the ferrite content in duplex stainless steel is increased and the 1:1 ratio is disturbed the steels become prone to pitting corrosion attack. This is the reason why Nickel is used in the filler material during welding as it is a austenite former and consequently helps in maintaining the austenite content in duplex stainless steels[10]. For maintaining the phase balance after welding sometimes post weld heat treatments i.e. solution annealing is done[11]. Heating and cooling rates during welding also play a vital role in maintaining the ratio of both the phases in duplex stainless steel[10,12].

One of the major problems in DSS is the formation of intermetallic phases. These intermetallic phase are often responsible for detoriating not only the mechanical properties but the corrosion properties too. These phases are induced in duplex stainless steels during welding, improper heat treatments and prolonged heating at high temperatures. There are various intermetallic phases that precipitate at different temperatures in duplex stailess steels.

Intermetallic phases	Chemical formula	Temperature range(°C)
Sigma(σ)	Fe-Cr-Mo	600-1000
Chi(χ)	Fe_{36}-Cr_{12}-Mo_{10}	700-900
Nitrides	CrN/Cr_2N	700-900
Carbides	M_7C_3/$M_{23}C_6$	550-650
R phase	Fe-Cr-Mo	550-800
Pie phase(π)	$Fe_7Mo_{13}N_4$	550-600
Alpha prime(α̍)	Fe-Cr	475

Table 8: Various intermetallic phases with their chemical compositions and temperature ranges[13]

Sigma phase(σ):

Sigma phase is a chromium and molybdenum rich precipitate which is hard in nature and is formed in the temperature range of 600-1000°C[14]. Sigma phase is non-magnetic in nature and is having a tetragonal structure. This phase is formed when ferrite in the matrix of duplex stainless steel is converted into secondary austenite and sigma phase. This is a eutectoid reaction and is displayed below:

$$\alpha \longrightarrow \gamma_2 + \sigma \qquad [15]$$

There are elements which increase the formation of sigma phase, they are as follow: Cr, Mo, Ni, Si, Mn. Sigma phase has the fastest precipitation rate in the temperature range of 850-900°C. Generally, sigma phase precipitates at the grain boundaries of α/α and α/γ grains[16]. Once the initiation of sigma phase is done, it propagates along the ferrite grain as the diffusion rate in ferrite phase is 100 times faster than that of austenite, hence making it a favourable site for other precipitates to initiate and grow[17].

Chi phase(χ):

Prior to sigma phase formation, chi phase formation takes place in the temperature range of 750-850°C. Chi phase forms at the interface of ferrite/ferrite grain boundaries and then ultimately propagates in the ferrite grains. Chi phase is rich in Mo content when compared with sigma phase[18].

Secondary austenite(γ_2):

Formation of secondary austenite in duplex stainless steels is not only in one temperature range or through one mechanism. Below 650°C formation of secondary austenite takes place through diffusion-less transformation. In the temperature range of 650-800°C, secondary austenite is in the form of widmanstatten austenite. In the temperature range of 800-900°C, formation of secondary austenite takes place through eutectoid reaction, from ferrite to sigma phase and secondary austenite[15].

$$\alpha \longrightarrow \gamma_2 + \sigma$$

Chromium nitrides(CrN/Cr_2N):

Chromium nitride CrN is formed during welding in the heat affected zones due to improper heat treatment operations. Chromium nitride Cr_2N is formed at inter-granular sites this happens during fast cooling from high annealing temperatures. These nitrides generally precipitate in the temperature range of 700-900°C[19].

R-phase:

R phase is a Mo rich precipitate and its stability increases with increase in Mo content. R-phase generally precipitates in the temperature range of 550-650°C. During the initial stages of ageing this phase is observed, but after some time this phase is transformed to sigma phase. R phase forms at inter and intra-granular sites[20].

Π-phase:

Similar to sigma phase, this phase is also rich in chromium and molybdenum contents. Formation of sigma phase takes place when isothermal heat treatment is done at 600°C for a long time[9].

τ-phase:

τ-phase has a needle like structure which is formed at the ferrite/ferrite grain boundaries after heat treatment in the temperature range of 550-650^{O}C[21].

Alpha prime phase(α̍):

This phase generally forms in the temperature range of 280-500°C. the presence of miscibility gap in Fe-Cr phase diagram causes this embrittlement in duplex stainless steel. The decomposition of ferrite into α-phase(iron rich phase) and α̍-phase(rich in chromium) takes place. This embrittlement is having a highest rate at 475°C, hence is also known as 475°C embrittlement[22].

$$\alpha \longrightarrow \alpha(\text{Fe-rich}) + \acute{\alpha}(\text{Cr-rich})$$

2.6 Regular duplex stainless steel 2205 grade

The most commonly used duplex stainless steel grade is 2205 or UNS S32205 or EN 1.4462. The 80% of the duplex stainless steel production is of 2205 grade. This grade of duplex stainless steel has better corrosion resistivity than austenitic 316 grade in similar environmental conditions. 2205 duplex grade also have an advantage of higher yield strength than 316 grade.

Grade	%C	%Mn	%P	%S	%Si	%Cr	%Ni	%Mo	%N	%Fe
2205	0.03	2.00	0.03	0.02	1.00	22-23	4.50-6.50	3-3.5	0.14-0.20	bal.

Table 9: Chemical composition of 2205 DSS grade[4]

Mechanical properties	UTS(MPa)	YS(MPa)	%El	Hardness(BHN)
2205 grade	655 min.	450 min.	25 min	293

Table 10: Mechanical properties of 2205 DSS grade[4]

2.7 General Characteristics of 2205

- PREN(Pitting resistance equivalent number) value for these stainless steels is 34. The formula for calculating PREN is as follows:

$$\text{PREN}_{16} = \%Cr + 3.3(\%\text{Mo}) + 16(\%\text{N})$$

- Carbon content in this grade is kept quite low to reduce the formation of carbides.

- Yield strength is as high as twice the austenitic stainless steel.
- It has good weldability with minimal inter-granular corrosion in as welded condition.
- It has high resistance to SCC in chloride and in hydrogen sulphide containing environments.
- Exhibits high resistance to corrosion fatigue, pitting and crevice corrosion and erosion-corrosion.

Machinability:

- Cutting procedures with high speed steel tools are same as for AISI 316.
- With carbide tipped tools, the cutting speeds should be 40% less than for AISI 316 in roughing operations and 20% less for finish machining.

Fabricability:

- Nearly twice the force is required to initiate plastic deformation compared to that required for AISI 304 and 316.
- Plastic deformation proceeds as easily as in austenitic stainless steel beyond yield strength.
- It can be cold bent to 25% deformation without requiring subsequent heat treatment.

Weldability:

It can be easily welded through Manual metal arc welding(MMAW).

Corrosion Resistance:

- It has better corrosion resistance as compared to AISI 316.
- Welded-joints easily pass inter-granular corrosion test
- Better resistance to pitting and crevice attack than 304 and 316 at higher temperatures and chloride contents.
- The combined high strength, hardness and corrosion resistance provide 2205 with superior corrosion fatigue and erosion/corrosion resistance.

Applications:

- Chemical industries- pumps, fans, centrifuges, sulphur melting coils, chemical tanks
- Pulp and paper industries- digester in sulphate and sulphite plants, blow tanks, blow lines
- Petrochemical industries
- Power generation industries
- Oil and gas industries
- Desalination
- Architecture and construction
- Food processing equipment
- Biofuel plants
- Cargo tanks for ships and trucks

2.8 Effect of copper(Cu) and tungsten(W) on duplex stainless steels

In the recent 15 years or so the current focus is on producing lean duplex grades of DSS having a bit inferior corrosion properties but with no compromise with the mechanical properties[23]. Some where around I was also having a same mind set before going for this project. Cu and/or W additions are considered to improve the corrosion resistance of this grade in specific solutions such as sulphuric acid mixtures. W was also considered to reduce the kinetics of precipitation of intermetallic phases. The addition of Cu and W come into picture when talking about higher grades of DSS to achieve higher PREN values[6].

Study of copper addition to various duplex stainless grade reduces the total amount of intermetallic compounds. In particular, addition of copper to the base alloy results in suppressing the amount of sigma phase whereas the amount of chi phase is also reduced to some extent. The presence of copper also decreases the Degree of sensitizaiton (DOS) due to the delayed precipitation of intermetallic compounds, when compared with that of the base alloy[24].

SDSS and HDSS contain large amounts of chromium and molybdenum contents and hence thses stainless steels have a greater tendency towards formation of intermetallic phases. Hence, for my project I have taken a standard 2205 duplex stainless steel so that the tendency of formation of intermetallic compounds must be done.

The precipitation rate of sigma phase is higher in case of SDSS and HDSS when compared with 2205 grade of duplex stainless steel, this was confirmed as it formed 1% sigma phase when aged for 2000 seconds at 850°C whereas 1% sigma phase formation has occurred when aged for 100 seconds at 850°C for SDSS[24].

One more advantage of adding copper to 2205 duplex stainless steel is when we are dealing with samples of large dimensions, the cooling rate during quenching is different at the interior of the sample i.e. it is quite low which gives a chance to sigma phase to precipitate at those low rates of cooling. But when copper is present in these steel then copper reduces the tendency of precipitation of sigma phase during slow cooling rates. This happens because of the fact that copper particles pinup the moving sigma phase boundaries[24].

Addition of copper also reduces the degree of depletion of Cr, Mo, and W. This happens because of the fact that formation of intermetallic phases is reduced and hence the degree of sensitization is also reduced. The corrosion property is also enhanced which is the most important property when talking about stainless steels.

Copper addition is obvious to improve the properties of duplex stainless steels, but when we keep on increasing the copper content then after 1.3-1.4% (by weight) of copper the pitting corrosion resistivity is affected. The pitting potential (Ep) values at different copper contents in 2205 duplex stainless steels are given below:

Ep of DSS = 889 Volt

Ep of $DSS_{Cu(1.3)}$ = 890 Volt

Ep of $DSS_{Cu(3)}$ = 575 Volt

The pitting potential values show a sudden decrease with increase in copper content and this decrease in pitting potential results in decrease in PREN values. Hence, the copper content is limited to 1.5% (by weight)[25].

In a study it was observed that addition of copper more than 1-1.2% (by weight) decreased the ferrite content of the duplex stainless steel by 8-10%. This is also one of the reason that why we are not adding copper more that 1.5% as it will then affect our ferrite phase stability and our ferrite to austenite ratio will be affected. Any difference in the ferrite to austenite ratio will adversely affect the properties of 2205 duplex stainless steel[26].

Tungsten addition in heat affected zone (HAZ) of DSS is effective in delaying the precipitation of sigma phase and the tendency of formation of Chi phase increases. This happens because with the addition of tungsten the nucleation efficiency of chi phase increases and also the growth rate of formation of sigma phase is lowered[27].

Tungsten can also be used as a substitute of molybdenum as tungsten in place of molybdenum will reduce the tendency of intermetallic phases which are rich in molybdenum[28].

In ferritic stainless steels, tungsten was added as a partial substitution to Mo. This not only increased the resistance to pitting corrosion of the alloy by a synergic contribution of Mo and W but also reduced the amount of precipitation of sigma phase in the alloys[29].

Tungsten is added in this steel to form its own precipitates at higher temperatures reducing the tendency of formation of detrimental sigma and chi phases.

Chapter 3

Gaps found and Research Question

3.1 Gaps found

The aim of the present study is to alloy 2205 grade with copper(1.3-1.5%) and tungsten(4-4.5%). As copper and tungsten will induce precipitation hardening during ageing at different temperatures. Along with precipitation hardening they reduce the tendency of degree of depletion of major alloying elements in stainless steels Cr and Mo. Study of Dynamic recrystallization behaviour at high strain rates in Gleeble for hot compression by varing parameters like temperatue and strain rate.

The work on dynamic recrystallization at high strain rates has not been carried out by varying these parameters along with simultaneous effect of precipitation hardening through micro-alloying.

3.2 Research Question: What is the problem you want to solve?

The aim of my study is to enhance the corrosion property pitting corrosion resistivity in major by alloying it with copper and tungsten. Not only this the rate of precipitation of detrimental sigma and chi phases are also tried to reduced after alloying of Cu and W as both these elements help in precipitation of chi phase first than the sigma phase. As sigma phase is the parent phase for precipitation of all other detrimental phases like-R phase, G-phase, pie phase, alpha prime phase. With the decrease in the precipitation of sigma phase the properties of the newly alloyed duplex stainless steels will not be affected with decreased amount of intermetallic phases. Study of dynamic recrystallization at high strain rates is not studied in 2205 grade DSS using Gleeble simulator.

Chapter 4

Experimental Procedure

The experimental procedure that is adopted in the present work has been discussed in the following sections :

- Material Selection.
- Chemical analysis of 2205 Duplex Stainless Steel (DSS).
- Casting for alloying 2205 DSS grade with copper (Cu) and tungsten (W).
- Chemical analysis of 2205 DSS grade after alloying.
- Forging and Rolling of the obtained ingot.
- Characterization study: XRD, Metallography, SEM, Hardness, and DSC analysis of the samples obtained after rolling.
- Solutionizing the samples and then quenching and aging at various temperatures and time to study the precipitation of various phases.
- Gleeble to study the controlled thermo mechanical treatment for dynamic recrystallization at varying temperatures and strain rate.

4.1 Material Selection

There are five types of stainless steels based on their room temperature microstructure and each type is sub divided into various grades based on the chemical composition and mechanical properties. Out of all those grades most widely and easily available grades were 304 and 316 austenitic stainless steel. But the more superior properties of duplex stainless steel attracted me to carry my research work on 2205 duplex stainless grade. Duplex stainless steel was selected on the basis of its brilliant properties like pitting and crevice corrosion resistivity, stress corrosion resistivity, good weldability, mechanical properties and its wide range of applications in power plants, desalination facilities, the marine industry, off-shore industries, food industries, chemical industries, paper industries, nuclear industries and in structural industries. Also it has a two-phase structure which helps us in getting a wide range of properties. Hence, I selected duplex stainless steel to be my material for research. The most popular and standard grade of duplexs stainless steel is 2205 grade which contains in general, 22% Cr and %% Ni. Jindal stainless steel is one of the largest manufacturer of stainless steels in India. Its plant in Hisar, Haryana is the lone manufacturer of this duplex stainless steel grade in India. Hence, I brought this 2205 duplex stainless steel grade from Jindal Stainless Steel Hisar Limited (JSHL), India.

Duplex stainless steel, obtained from industry was in the form of rectangular rolled sheets of dimension 292mm×235mm×6mm. There were total of 5 sheets and each sheet was around 1.5 kg approx.

(a) **(b)**

Fig. 7: (a) Jindal stainless steel (Hisar) Limited; (b)2205 DSS grade sheet

4.2 Chemical analysis of 2205 Duplex Stainless Steel (DSS) samples

A small sample of dimension 20mm×20mm×6mm was cut from the 2205 DSS sheet using an abrasive cutter(HITACHI 355 CUT OFF MACHINE, CC14SF(Silicon carbide blade)) at mechanical metallurgy workshop. And then into more small pieces through abrasive cutting machine at MRC. The chemical analysis of the sample was done using Optical Emission Spectrometer at Materials Research Centre, MNIT Jaipur.

(a) **(b)**

Fig. 8: (a),(b) Two different types of abrasive cutters.

Optical Emission Spectroscopy(OES), is a well trusted and widely used analytical technique used to determine the elemental composition of a broad range of metals. The type of samples which can be tested using OES include samples from the melt, primary and secondary metal production, and in the metals processing industries, tubes, bolts, rods, wires,

plates and many more. The part of the electromagnetic spectrum which is used by OES includes the visible spectrum and part of the ultraviolet spectrum. In terms of wavelength, that's from 130 nanometers upto around 800 nanometers. OES can analyse a wide range of elements from Lithium to Uranium in solid metal examples covering a wide concentration range, giving very high accuracy, high precision and low detection limits. The elements and concentrations that OES analyzers can determine depend on the material being tested and the type of analyzer used.

OES analyzer contains three major components, the first is an electrical source to excite atoms within a metallic sample so that they emit characteristics light, or optical emission, lines- requires a small part of the sample to be heated to thousands of degrees Celsius. This is done using an electrical high voltage source in the spectrometer via an electrode. The difference in electrical potential between the sample and electrode produces an electrical discharge, this discharge passes through the sample, heating and vaporizing the material at the surface and exciting the atoms of the material, which then emits the element-characteristics emission lines. Two forms of electrical discharge can be generated, either an arc which is an on/off event similar to a lightening strike, or a spark-a series of multi-discharge events where the voltage of the electrode is switched on and off. There two modes of operation are used depending on the element measured and the accuracy required. The second component is an optical system. The light, the multiple optical emission lines from the vaporized sample known as a plasma pass into the spectrometer. A diffraction grading in the spectrometer separates the incoming light into element-specific wavelengths and a corresponding detector measures the intensity of light for each wavelength. The intensity measured is proportional to the concentration offset element in the sample. The third component is a computer system. The computer system acquires the measured intensities and processes this data via a predefined calibration to produce elemental concentrations. The user interface ensures minimal operator intervention with results clearly displayed which can be printed or stored for future reference.

When energy of an electrical discharge interacts with an atom, some of the electrons in the atom's outer-shell electrons are less tightly bound to the nucleus of the atom because they are further away from the nucleus and so require less input energy to be ejected. The ejected electrons create a vacancy making the atom unstable. To restore stability, electrons from higher orbits further away from the nucleus drop down to fill the vacancy. The excess energy released as the electrons move between the two energy levels or shell is emitted in the form of element-specific light or optical emission. Every element emits a series of spectral lines corresponding to the different electron transitions between the different energy levels or shells. Each transition produce a specific optical emission line with a fixed wavelength or energy of radiation. For a typical metallic sample containing iron, manganese, chromium, nickel, vanadium, etc, each element emits many wavelengths, leading to a line-rich spectrum. For example, iron emits just over 8000 different wavelengths so choosing the optical emission line for a given element in a sample is important. The characteristic light emitted by the atoms in the sample is transferred to the optical system where it splits into its spectral wavelengths by the high-tech grading, the grading contains upto 3600 grooves per millimetre.

Next the individual spectral line peak signals are collected by detectors and processed to generate spectrum showing the light intensity peaks versus their wavelengths. This means that OES provides qualitative information about the sample measured; however, OES is also a quantitative technique. As we can see, the peak wavelength identifies the element, and its peak area or intensity gives an indication of its quantity in the sample. The analyzer then uses this information to calculate the sample's elemental composition based on a calibration with certified reference material. The whole process, from pressing a start button or a trigger to getting the analysis results, can be quick as 3 seconds or it can take upto 30 seconds for a full accurate quantitative analysis, it all depends on the analyser used, the range of elements measured and the concentrations of those elements.

Fig. 9: OES(Optical Emission Spectroscopy)

Element(%) S.No.	%C	%Mn	%Si	%S	%P	%Cr	%Ni	%Mo	%Cu	%W
Sample	0.0517	0.657	0.468	0.0	0.0232	21.2	4.34	2.86	0.055	0.0213

Chemical composition continue:-

	%Al	%As	%B	%V	%Sn	%Co	%Ti	%Nb	%Fe
Sample	0.0073	0.0145	0.0012	0.0670	0.0087	0.0	0.0	0.0	70.1

Table 11: Chemical composition of 2205 grade of duplex stainless steel(wt%)

4.3 Casting for alloying 2205 DSS grade with copper (Cu) and tungsten (W)

Duplex stainless steel sheets were cut into small pieces so that they can fit into the crucible used for casting. Crucible which was used for performing the duplex stainless steel casting were imported from China. It was not normal ceramic crucibles. The crucible is known as China crucible. This crucible was selected as the performed trail castings on graphite crucible picks carbon which is very much detrimental for duplex stainless steel and magnesia crucible was not able to sustain such high temperatures required for melting 2205 grade of duplex stainless steel, magnesia crucible was fractured from the bottom during casting. It is a ceramic crucible but the composition was not revealed by the company. Casting was performed in a induction furnace.

Fig. 10: China crucible

Fig. 11: Setup of Induction furnace with chillar

Copper was in the form of solid with 99.99% purity and Tungsten was in the form of ferro-tungsten with 75% of tungsten by weight.

According to the composition decided the amounts of copper and tungsten were added to make a 2kg casting. The amount of copper taken was 27.368gm and ferro-tungsten was 120gm and the rest was duplex stainless steel to cast a 2kg ingot.

Mould used for pouring the molten metal was a tool steel mould.

Element(%) S.No.	%C	%Mn	%Si	%S	%P	%Cr	%Ni	%Mo	%Cu	%W
Sample	0.0771	0.434	0.584	0.0	0.027	20.1	4.38	2.83	1.44	4.52

Chemical composition continue:-

	%Al	%As	%B	%V	%Sn	%Co	%Ti	%Nb	%Fe
Sample 1	0.0035	0.0138	0.0028	0.0972	0.0091	0.0	0.0002	0.05	65.3

Table 12: Chemical composition of alloyed 2205 DSS grade after casting (wt%)

Hot Forging and rolling operations were performed on the obtained ingot after casting. Drop forging was done whereas two high rolling was done.

4.4 Characterization studies for 2205 duplex stainless steel after alloying through casting, forging and rolling

4.4.1 X-ray diffraction(XRD)

XRD is used to determine the crystal structure. It is based on the principle of Bragg's law($n\lambda=2d\sin\theta$) that describes how the angle of diffraction(θ) of an X-ray beam focused on a crystal is related to wavelength (λ) and inter-planar spacing (d). The presence of amorphous phases cannot be understood by X-ray diffraction technique. This is one of the major drawback of X-ray diffraction technique. XRD experiments were performed in the 2θ range of 20°-90° using Cu K_α target at the scan rate of 1°/min. XRD was done at IIT Kanpur and the data was analysed using X-pert software and then plotted using Origin software.

Fig. 12: X-ray Diffraction machine

X-ray diffraction(XRD) is an extensively used, it is a non-distructive technique for basic investigation of the crystal structure of materials. In the current analysis, two phase structure was clearly identified though XRD. The technique is based on the diffraction of an incident X-ray beam from the atomic planes of a crystal. The interference of coherent scattering planes causes intensity maxima of the diffracted radiation in dependence on the scattering angle. These maxima are known as diffraction peaks or also Bragg reflections. The scattering angle 2θ which the diffraction peaks or also Bragg reflections. The scattering angle 2θ where the diffraction peaks occur is given by the Bragg's law:

$$2d\sin\theta= n\lambda$$

Where d is the lattice spacing (the planar distance in the crystal lattice), λ is the wavelength of the X-rays and n is the diffraction order. For a polycrystalline material with random orientation of the crystallites the diffraction does not depend on sample orientation.

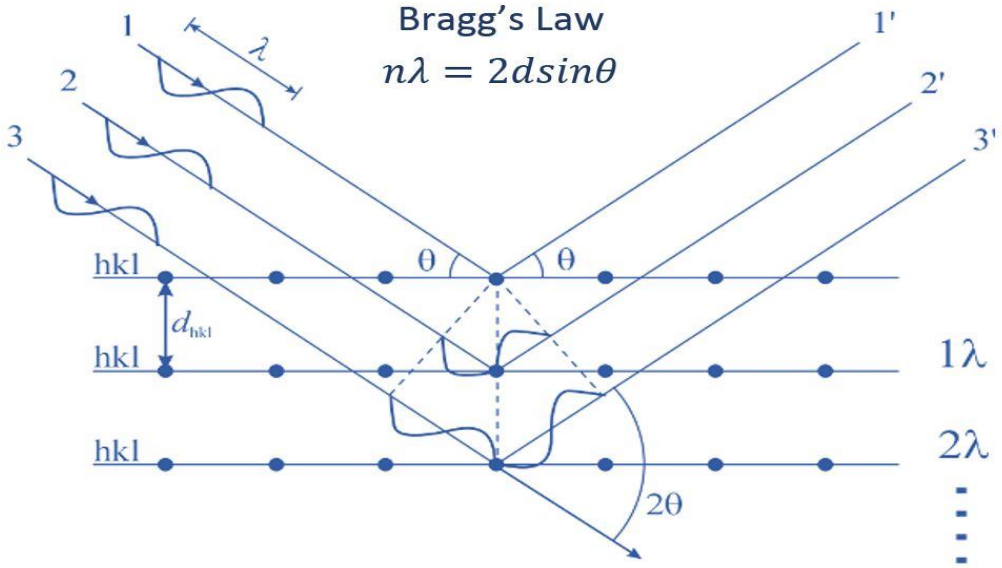

Fig. 13: Principle of X-ray diffraction

The X-ray diffraction beam is directed at a small incident angle $\theta_{in} < 1°$ to the sample surface in order to limit the penetration depth and to enhance the diffraction peaks obtained from the layer with respect to these from the substrate. The detector is moved along a circle around a sample, where the angle between the incident beam and the detector is denoted as 2θ. The measured property is the diffracted beam intensity (I) in dependence of the diffraction angle. From the obtained diffraction pattern following information can be obtained:

1. The distance between the crystal planes {hkl} (h, k, l- Miller indices) in the lattice and the lattice constants can be calculated from the position of the diffraction peaks. The phases can be determined by the comparison of these values with the standard sample. If the intensity relations of the Bragg are found to be different compared to the PDF data, then preferred crystallite orientation(texture) exists in the layer.

2. A shift of the diffraction angles from the tabulated positions is an indication that the crystal lattice is expanded, whereas a shift of the diffraction angle to larger values corresponds to a compression of the lattice. From the shift of the diffraction angles with the shift of the diffraction angles with sample orientation, information about macroscopic strains acting in the layer can be obtained.

3. From the broadening of the diffraction peaks of polycrystalline material the average grain size of the crystallite and microscopic strains in the layer can be determined. Diffraction peaks obtained from a perfect single crystal are very narrow.

4.4.2 Differential Scanning Calorimetry(DSC)

Differential scanning calorimetry (DSC) is a thermo-analytical technique which measures the heat into or out of a specimen. A DSC measures the heat of specimen with respect to a relative sample which is also taken and heated with the specimen, this relative sample is known as the reference sample. A differential scanning calorimeter heats the sample with a linear temperature ramp. DSC is a technique in which the difference in the amount of heat required to increase the temperature of a sample and reference are measured as function of temperature. Specimen sample and reference sample are both maintained at same temperature during the experiment. In DSC analysis, the temperature increases linearly with time using a temperature program. For DSC analysis, generally 10mg sample is taken, this is the major advantage of this experiment. DSC is the most widely used thermal analysis technique because of its user friendly technique. It gives results within few hours and the results obtained are quite reliable.

When there is physical transformation in the specimen sample like phase change or melting then some heat is more or less required to flow through the reference sample. This is done to maintaion both the samples at the same temperature. How much heat is needed to flow to the reference sample depends whether the process is exothermic or endothermic. In general, during melting of a solid sample more heat is needed to flow to the reference sample this is needed to increase the temperature of the reference sample to maintain the temperature of both the samples. As during melting the reference sample is absorbing heat hence we can say that melting of any specimen is a endothermic process. Similarly, if less heat is reuired to maintainthe temperature then the process is exothermic in nature. DSC measures the amount of heat absorbed or released by observing the heat flow between sample and reference[30].

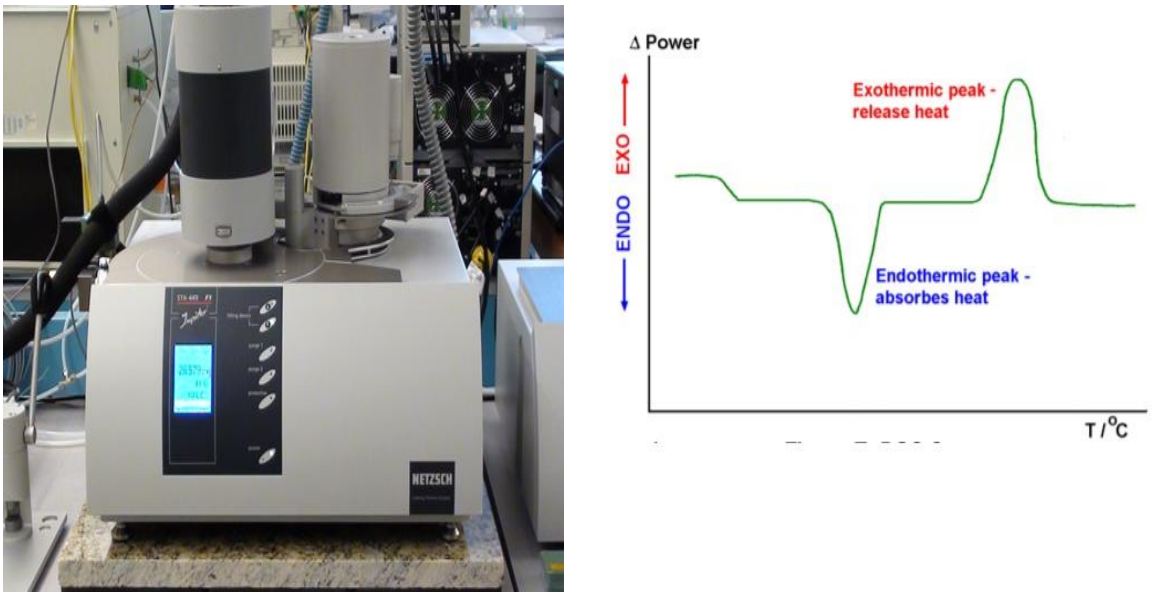

(a) **(b)**

Fig. 14: (a) Setup of DSC, (b) DSC curve showing exothermic and endothermic peaks

4.4.3 Optical Microscopy

In this a horizontal beam of light from some light source is reflected, by means of a plane gless reflector, downward through the microscope objective onto the surface of the specimen.

Fig. 15: Optical Microscope

Some of the incident light reflected from the specimen surface will be magnified in passing through the lower lens system, the objective; and will continue upward through the plane glass reflector and can be magnified again by the upper lens system, the eyepiece.

Metallographic study was carried out by adopting usual methods of paper polishing on 120, 320,400,600,800,1000,1200,1500,2000 papers followed by fine polishing in cloths with diamond suspensions of 6 µm, 3 µm, 1µm respectively. These polishing operations were performed on double disc polishing machine. In this process, scratches were removed and a polished surface just like mirror is obtained.

Fig. 16: Double disc polishing machine

Fig. 17: Diamond Suspensions

After the polishing samples were etched using a freshly prepared solution of $FeCl_3$, $CuCl_2$, HCl, Methanol and Nitric acid in the composition of 8.5gm, 2.4gm, 122ml, 122ml and 6ml respectively.

4.4.4 Scanning Electron Microscopy (SEM)

A scanning electron microscope (SEM) scans a concentrated electron beam over a surface to build an image. The electrons in the beam interact with the sample, producing different types of signals that can be utilized to gain information about the surface topography and composition. The SEM is a microscope that uses electrons instead of light to form an image.

The scanning electron microscope has many advantages over traditional microscopes. The SEM has a large depth of field, which permits more of a specimen to be in focus at one time. The SEM also has much higher resolution, so closely spaced specimens can be magnified at much higher levels [31]. Because the SEM uses electromagnets rather than lenses, the researcher has much more control in the degree of magnification. All of these advantages, as well as the actual strikingly clear images, make the scanning electron microscope one of the most useful instruments in research today [31].

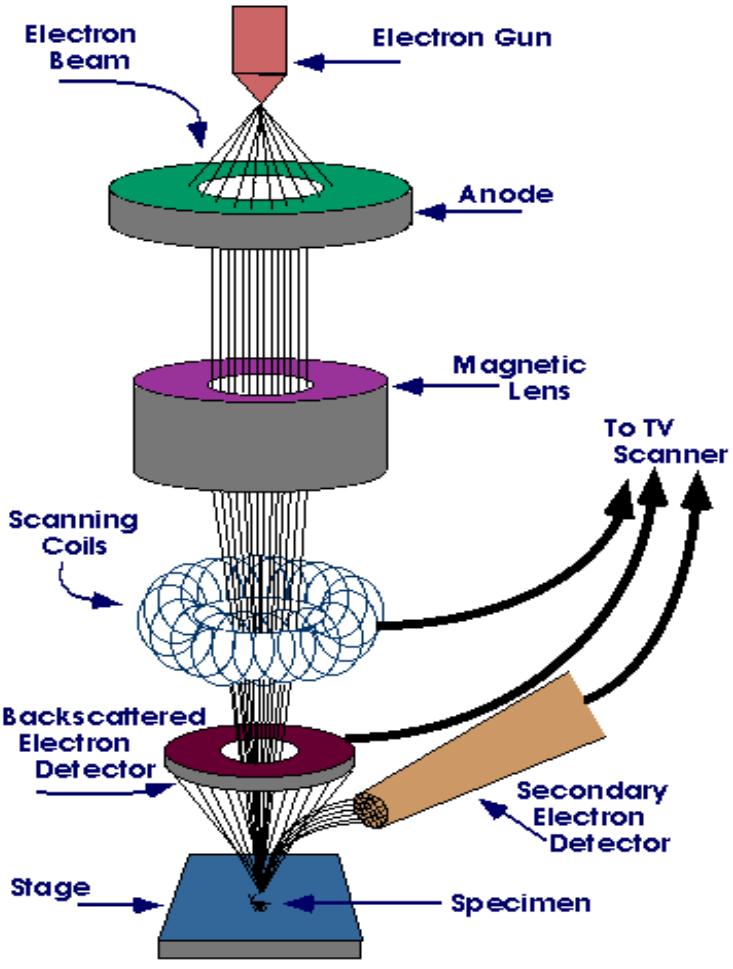

Fig. 18: Schematic of function of SEM

The most common SEM mode is the detection of secondary electrons emitted by atoms excited by the electron beam. The number of secondary electrons that can be detected depends, among other things, on specimen topography. By scanning the sample and

collecting the secondary electrons that are emitted using a special detector, an image displaying the topography of the surface is created. The signals used by a scanning electron microscope to produce an image result from interactions of the electron beam with atoms at various depths within the sample. Various types of signals are produced including secondary electrons (SE), reflected or back-scattered electrons (BSE), characteristic X-rays and light (cathodoluminescence) (CL), absorbed current (specimen current) and transmitted electrons. Secondary electron detectors are standard equipment in all SEMs, but it is rare that a single machine would have detectors for all other possible signals. Due to the very narrow electron beam, SEM micrographs have a large depth of field yielding a characteristic three-dimensional appearance useful for understanding the surface structure of a sample [31].

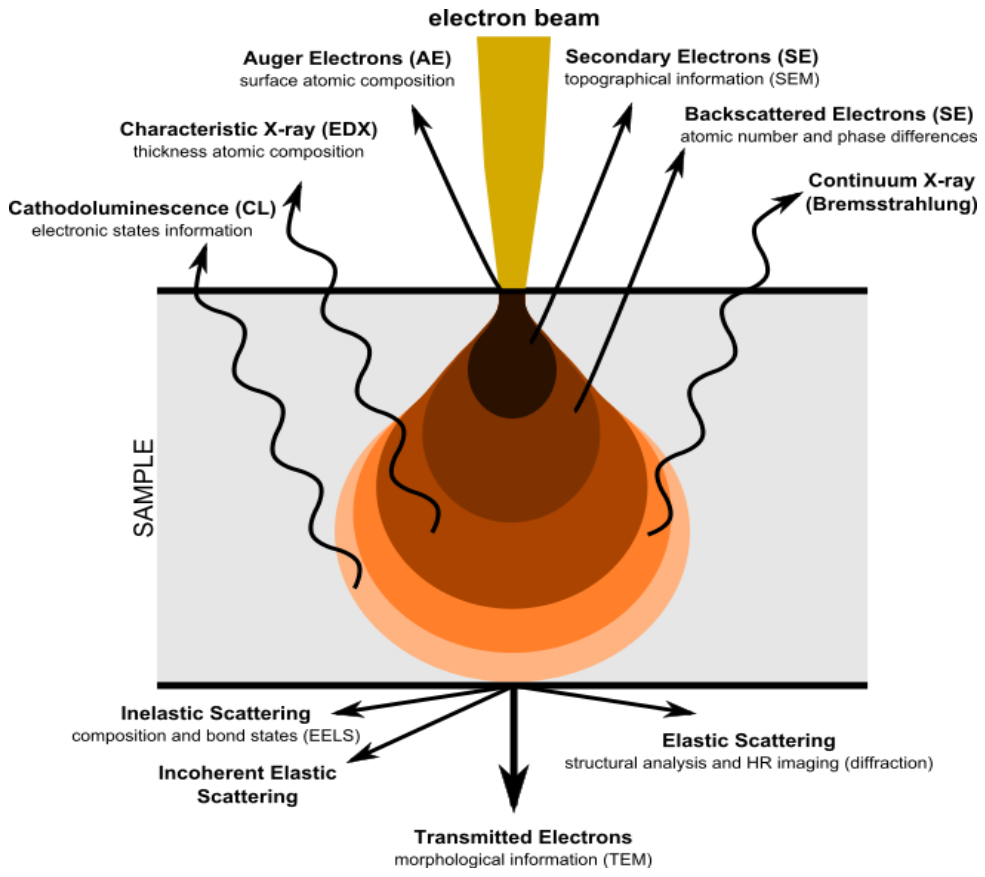

Fig. 19: Schematic of signals emitted from different parts of the interaction volume

In a typical SEM, an electron beam is thermionically emitted from an electron gun fitted with a tungsten filament cathode. Tungsten is normally used in thermionic electron guns because it has the highest melting point and lowest vapor pressure of all metals, thereby allowing it to be electrically heated for electron emission, and because of its low cost. Other types of electron lanthanum Hex boride cathodes, which can be used in a standard tungsten filament SEM if the vacuum system is upgraded or field emission guns (FEG), which may be of the cold-cathode type using tungsten single crystal emitters or the thermally assisted Schottky type, that use emitters of zirconium oxide [32].

The electron beam, which typically has an energy ranging from 0.2 keV to 40 keV, is focused by one or two condenser lenses to a spot about 0.4 nm to 5 nm in diameter. The beam passes through pairs of scanning coils or pairs of deflector plates in the electron column, typically in the final lens, which deflects the beam in the *x* and *y*-axes so that it scans in a raster fashion over a rectangular area of the sample surface.

Samples for SEM have to be prepared to withstand the vacuum conditions and high energy beam of electrons and have to be of a size that will fit on the specimen stage. Samples are generally mounted rigidly to a specimen holder or stub using a conductive adhesive. SEM is used extensively for defect analysis of semiconductor wafers, and manufacturers make instruments that can examine any part of a 300 mm semiconductor wafer. Many instruments have chambers that can tilt an object of that size to 45° and provide continuous 360° rotation.

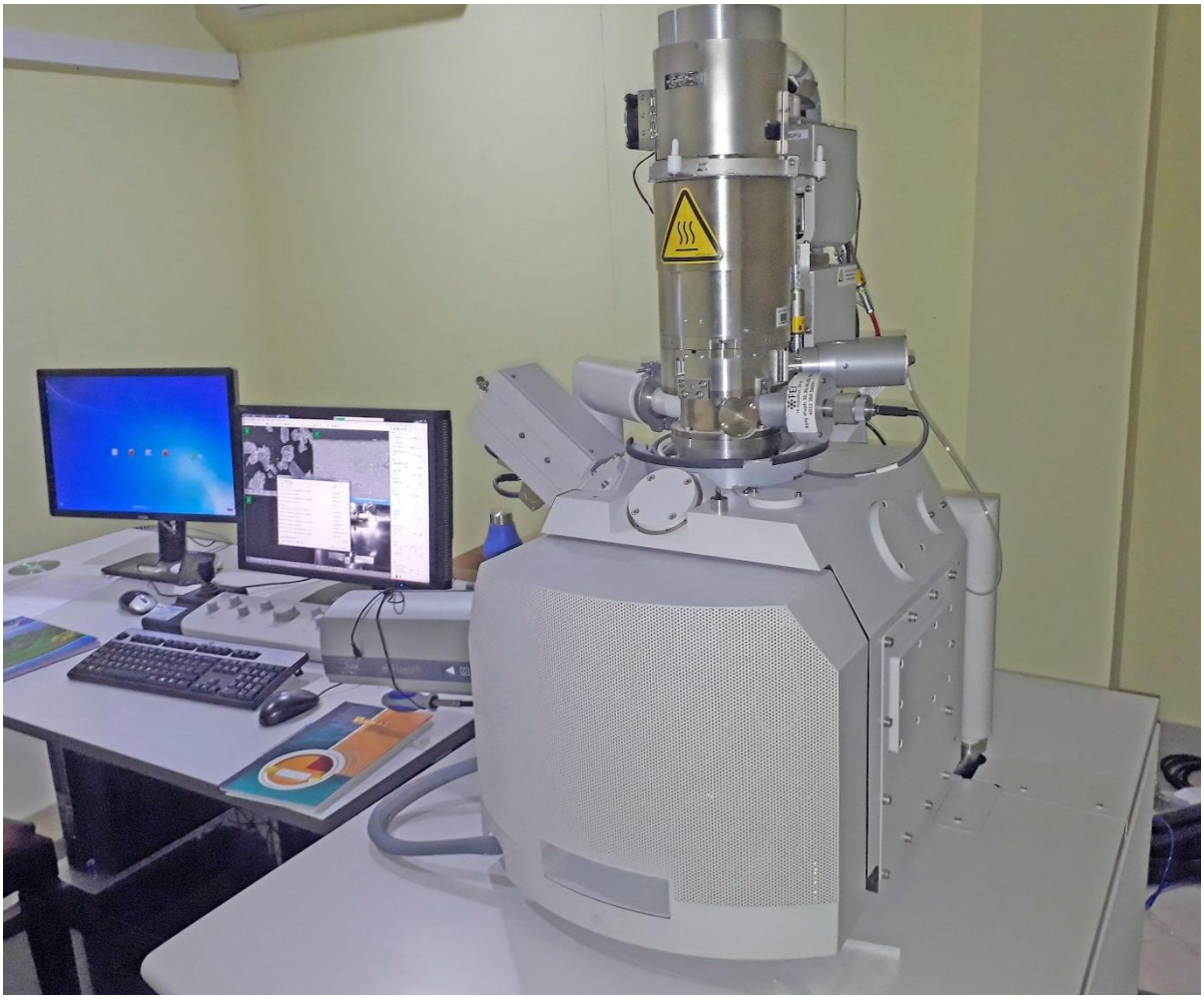

Fig. 20: Photographic view of SEM machine

4.4.5 Hardness measurement

The Vickers method is based on an optical measurement system. The microhardness test procedure, specifies a range of lights load using a diamond indenter to make an indentation which is measured and converted to a hardness value. The samples were first polished to obtain a clean and plain surface. After that, a load of 30 kg was applied to the specimen for 10 sec for measuring the hardness.

Each hardness value is the mean of 4 indentations. Hardness number is calculated by using formula given below,

$$HV = \frac{F}{A} \approx \frac{1.8544F}{d^2} \quad [\mathrm{kgf/mm^2}]$$

Where F= indentation force (Kgf)

D= Average length of diagonals of indent formed (mm)

Fig. 21: Micro Vickers hardness tester

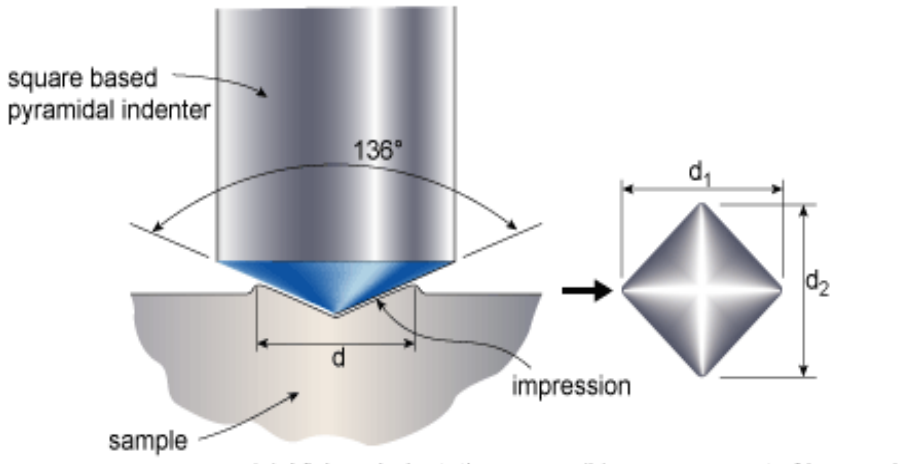

Fig. 22: Schematic of micro-Vickers hardness

4.4.6 Gleeble 3800 Simulator

Thermal-Mechanical Physical Simulation System

Fig. 23: Gleeble Simulator

Gleeble 3800 is a thermal and mechanical testing system which is fully integrated and digitally controlled. It has a user friendly windows based software and is attached to a computer to store data and give input parameters. It is combined with an array of powerful processors which provides an extremely user-friendly interface to create, run and analyze data from thermal-mechanical tests and physical simulation programs.

The experiments which are performed on Gleeble are 8-10 times more accurate than tests performed on other machines or instruments and the results so obtained are also more accurate.

Performance parameters	Gleeble 3800
Maximum heating rate	10,000°C
Maximum quenching rate	10,000°C
Maximum stroke	125 mm
Maximum stroke rate	2000 mm/sec
Minimum stroke rate	0.001mm/sec
Maximum force	20 tonnes
Maximum specimen size	20mm daimeter

Table 13: Various parameters in Gleeble with their limits

Hydrawedge Gleeble system is used for performing hot compression tests at strain rates of 1 and above. For my strain rates this hydrawedge attachment was used.

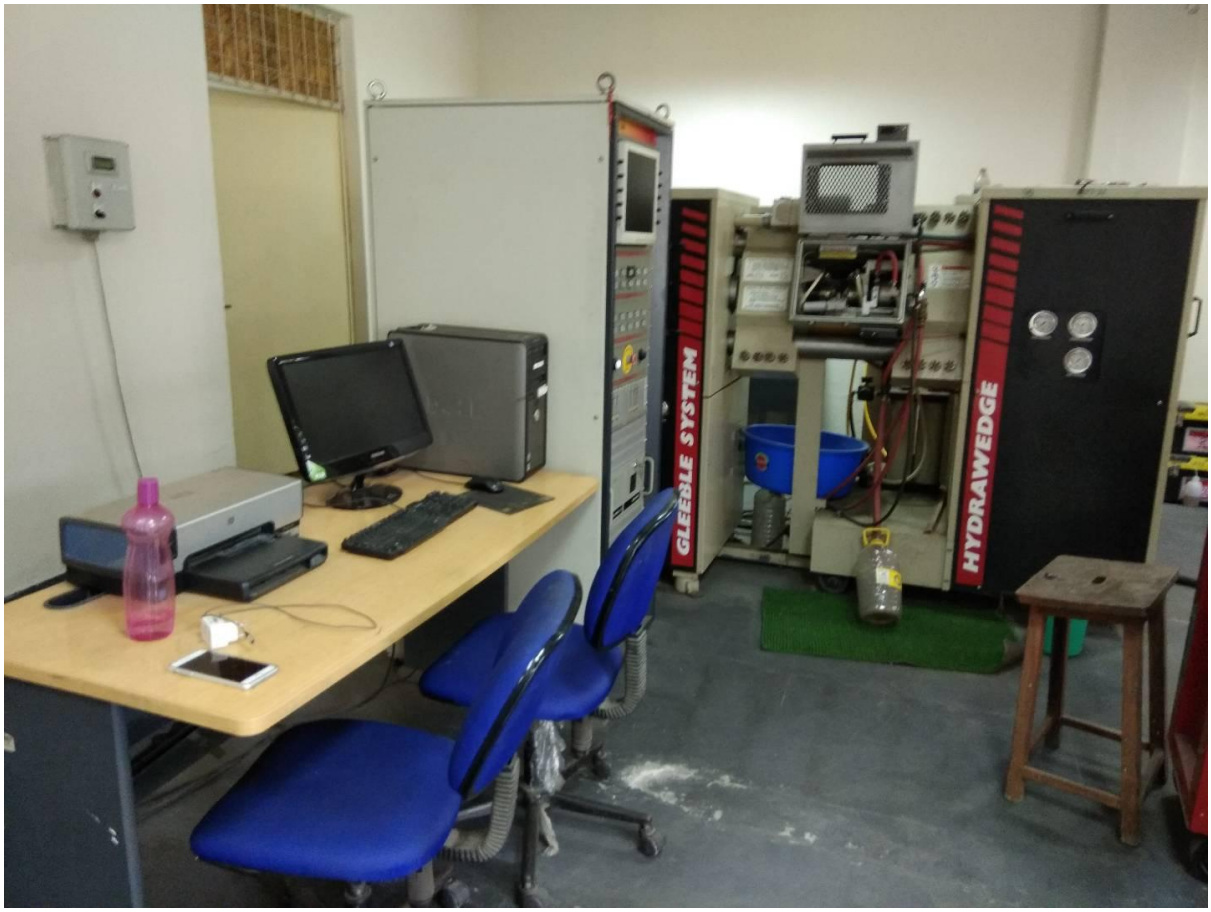

Fig. 24: Setup of Gleeble 3800 with Hydrawedge at IIT Roorkee

The heating system of the Gleeble 3800 is direct resistance heating and it has a tendency of heating the specimens at rates upto 10,000°C/second. Gleeble 3800 can hold and temperature needed during different operations. The grips which are used to hold the specimen are made up of tungsten carbide then a graphite coating is used and then copper plate is used for fast heat conduction. Graphite coating is used in between to avoid fusing. These high thermal conductivity grips and copper plate makes gleeble capable of high heating and cooling rates on the specimen surface.

Thermocouples are spot welded onto the specimen itself and hence there is more accuracy when talking about the sample temperatures. As gleeble is having a unique designed heating system, the thermal tests performed on it are having 8 to 10 times more accuracy than conventional furnaces.

There is an option of either of either induction heating or resistance heating. Induction heating is well suited for uniaxial compression testing(flow stress). The highest capacity of 10,000°C/sec is achieved using a direct resistance heating system. Both the heating systems are fully integrated to work on the Gleeble as well as on the software.

The Gleeble 3800 mechanical system is a fully integrated hydraulic system which is capable of exerting as much as 20 tons of static force in compression or 10 tons in tension, with an available upgrade of 20 tons of static load in tension. Displacement rates as fast as 2000mm/second can be achieved using Gleeble 3800.

The data input system for mechanical testing allows the operator to switch between the control variables at any time and as often as required during the test. Control modes available during the test modes are stroke displacement, force, various extensometers, true stress, true strain, engineering stress, and engineering strain.

Tests than can be performed using Gleeble 3800 are listed below:

- Hot/warm tensile testing on many different specimen geometries
- Hot/warm compression testing
- Uniaxial compression
- Plane strain compression
- Strain Induced Crack Opening(SICO)
- Develop stress vs strain curves
- Melting and solidification
- Nil strength testing
- Hot ductility testing
- Thermal cycling/heat treatment
- Dilatometry/phase transformation
    - On heating/ cooling
    - Continuous/ non-continuous
    - Isothermal

    - Post deformation
- Stress relaxation studies
- Creep/ stress rupture
- Fatigue
    - Thermal fatigue
    - Thermal/mechanical fatigue

Different processes that can be performed using Gleeble3800 are as follows:

- Continuous casting
- Mushy zone processing
- Hot rolling
- Forging
- Extrusion
- Weld HAZ cycles
- Upset butt welding
- Diffusion bonding
- Continuous strip annealing
- Heat treating
- Quenching
- Powder metallurgy/sintering

Gleeble 3800 system is available with various Mobile Conversion units (MCU's) which include a test chamber with grips and are mounted on wheels so that one MCU may be detached away from the Gleeble and another MCU configuration can be used. Each MCU offers unique testing and simulation capabilities and can be added to the Gleeble 3800.

Different Mobile Converson Units are discussed below:

General Purpose MCU: it is a standard MCU of Gleeble 3800 system, this unit is used for both tension and compression capabilities and a wide range of grips are available for different types of samples.

Hydrawedge: This is one of the most important MCU of Gleeble 3800 system. Hot rolling and forging processes are easily performed on Hydrawedge. Multiple-hit, high speed deformations are performed on Hydrawedge. With independent control of strain and strain rate and a mechanical stop to eliminate deformation overshoot.

Hot Torsion: The Hot Torsion Mobile Conversion Unit (MCU) is capable of applying torque up to 100 Nm (50 Nm standard configuration) and test specimens can be heated or quenched at any time during the test, which makes it very flexible for research purpose.

The cooling system of Gleeble 3800 is equipped with two Quenching units named as Quench 1 and Quench 2.These quench tanks are placed at the back of the hydrawedge MCU. The water is directly used for quenching the samples during the test. We need to fill the water tanks manually after every test is performed.

Fig. 25: Sample quenching setup of Gleeble 3800

Input parameters used for Hot compression test in Gleeble 3800:

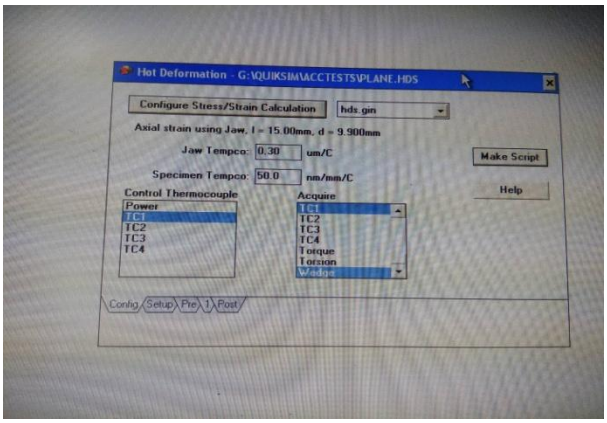

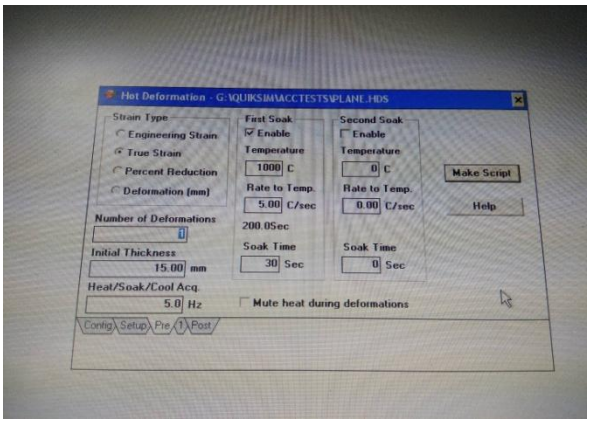

(a) **(b)**

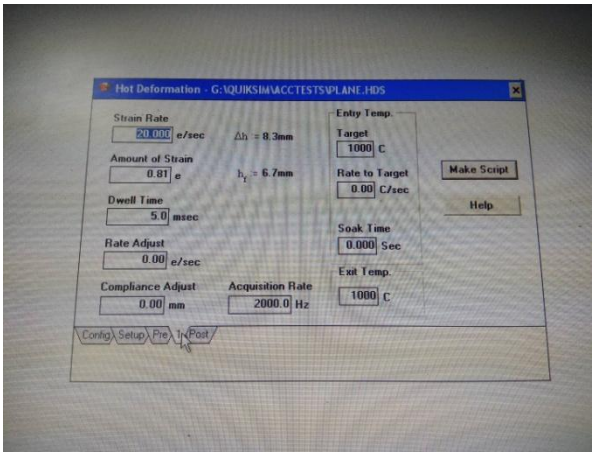

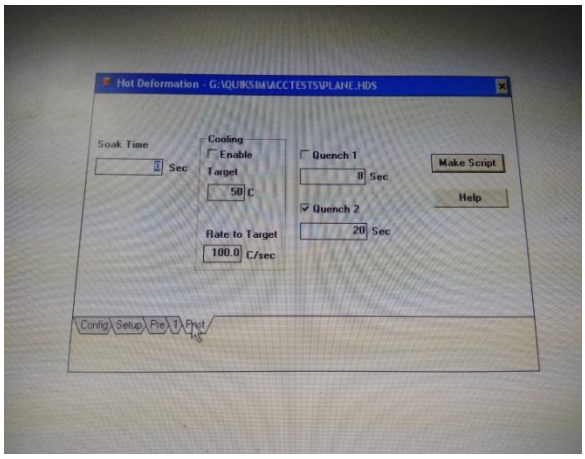

(c) **(d)**

Fig. 26: Input parameters for Hot compression test in Gleeble 3800

Before the start of the experiment there are following parameters which we need to set for proper working of the test to be performed. Fig 26(a) shows input parameters on the test to be performed on Gleeble and the details of thermocouple connected to the system. Fig (b) shows the input parameters like Strain type, Temperature to be heated, rate of heating and soaking time. Fig (c) shows the input parameters like stain rate, amount of strain, input temperature and exit temperature of the sample. Fig (d) shows the details of quenching system i.e. which quenching system to be used.

For hot compression test in Gleeble the sample size was 10mm×10mm×15mm.

Chapter 5

Results and Discussion

2205 grade, Duplex stainless steel contains a dual phase structure i.e. ferrite and austenite with approximately 50-50%. Because of the presence of both the phases this steel itself becomes special as it has the properties of both the phases. DSS are generally used for various applications in oil, chemical, marine and petrochemical applications, particularly where chlorides are present.

5.1 Base material and its mechanical properties

The initial microstructure of the bas material i.e. 2205 grade duplex stainless steel is shown below:

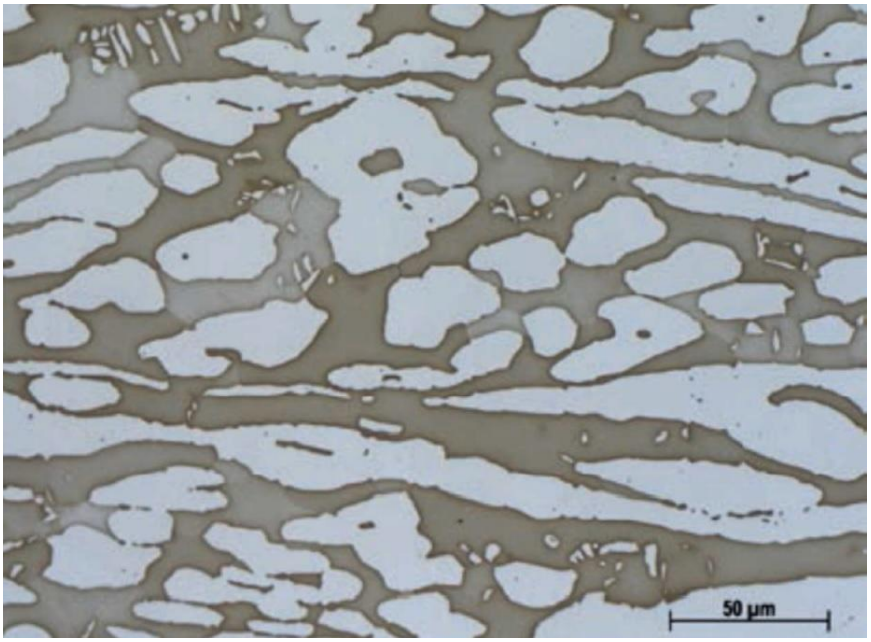

Fig. 27: Microstructure of 2205 duplex stainless steel grade

The microstructure clearly shows a two phase structure that contains ferrite and austenite in almost equal amounts. The dark region in the a ferrite matrix and the light region in the microstructure is austenite. This is because it contains both austenite and ferrite forming elements and these elements stabilize both the phases at room temperature. The stabilization of the phases is studied by the schaeffler diagram.

The Schaeffler diagram is generally used to depict the phases present in an alloy as a function of nickel and chromium equivalents.

There formulae used for calculating the nickel and chromium equivalents in present case are given below:

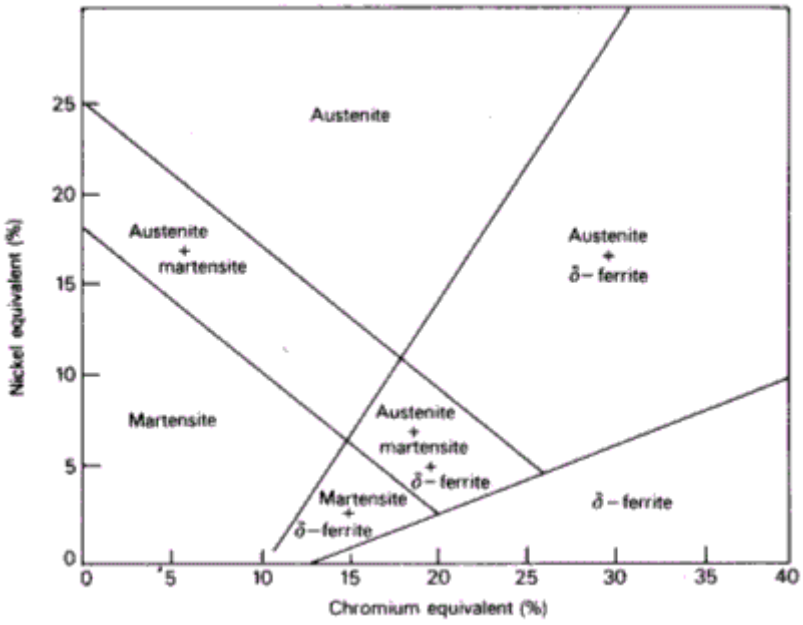

Fig. 28: Schaeffler Diagram

Chromium equivalent = (%Cr) + 2 (%Si) + 1.5 (%Mo) + 5 (%V) + 5.5 (%Al) + 1.75 (%Nb) + 1.5 (%Ti) + 0.75 (%W) …… **(1)**

Nickel equivalent = (% Ni) + (% Co) + 0.5 (%Mn) + 0.3 (%Cu) + 30 (% C) + 25 (% N)...**(2)**

The values in equations 1 and 2 above are in weight percentage.
From the schaeffler diagram it is clear that Duplex stainless steel belong to which region.

Mechanical properties	UTS(MPa)	YS(MPa)	%El	Hardness(BHN)
2205 grade	655 min.	450 min.	25 min	293

5.2 Chemical composition of the initial 2205 grade of duplex stainless steel

Grade	%C	%Mn	%P	%S	%Si	%Cr	%Ni	%Mo	%N	%Fe
2205	0.03	2.00	0.03	0.02	1.00	22-23	4.50-6.50	3-3.5	0.14-0.20	bal.

Pitting resistance Equivalent number(PREN) is the measure of resistivity of any stainless steel towards pitting. Pren is calculated using formulae as follows:

$$PREN_{16} = \%Cr + 3.3(\%Mo + 0.5(\%W)) + 16(\%N) \ldots\ldots (3)$$

$$PREN_{30} = \%Cr + 3.3(\%Mo + 0.5(\%W)) + 30(\%N) \ldots\ldots (4)$$

From the above formula (3), the initial PREN value which is observed is approx 33.48.and this value is quite low when we talk about pitting resistivity hence we have added tungsten(W) to it which will increase its PREN value. We could have also added Mo as it 3.3 times more resistant to pitting than chromium but addition of molybdenum increases the tendency of this steel towards the formation of intermetallic phases which are highly

detrimental for our steel during its applications. The PREN value after the addition of Tungsten(4.52% by weight) increased to 39.368.

Casting was done in Induction furnace for alloying copper and tungsten in 2205 duplex stainless steel. The ingot obtained from casting was then forged and rolled to improve its mechanical properties. Results of OES after the casting are as follows:

Element(%) S.No.	%C	%Mn	%Si	%S	%P	%Cr	%Ni	%Mo	%Cu	%W
Sample	0.0771	0.434	0.584	0.0	0.027	20.1	4.38	2.83	1.44	4.52

	%Al	%As	%B	%V	%Sn	%Co	%Ti	%Nb	%Fe
Sample 1	0.0035	0.0138	0.0028	0.0972	0.0091	0.0	0.0002	0.05	65.3

Table 14: Chemical composition of alloyed 2205 DSS grade after casting (wt%)

The desired composition is achieved and now the characterization is done to see the properties. The tests that are followed are as follows:

5.3 X-ray diffraction

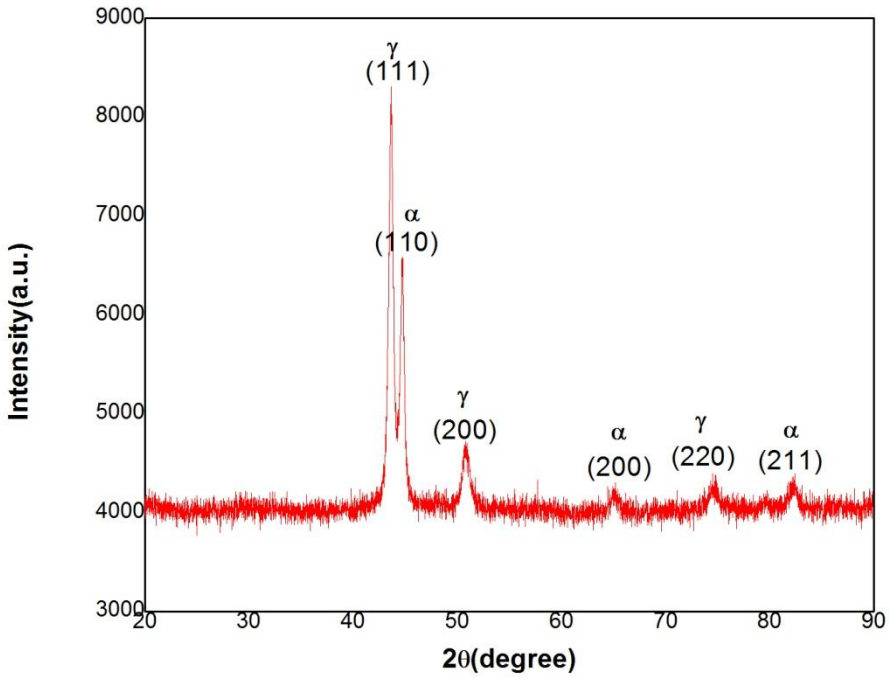

Fig. 29: XRD analysis show the two phases present in alloyed 2205 DSS

The X-ray diffraction pattern clearly shows the presence of two phases. These two phases are austenite and ferrite. The **JCPDS** (Joint Committee on Powder Diffraction Standards) **card**

was used for analysing the data and after matching the peaks with standard peaks, they were identified as austenite and ferrite phase peaks. Austenite is having face-centered cubic (fcc) lattice whereas ferrite phase is having body centred cubic (bcc) lattice. X-ray diffraction study was performed at IIT Kanpur. The X-ray diffraction pattern was observed in the 2θ range 0f 20°-90°.

5.4 Optical Microscopy

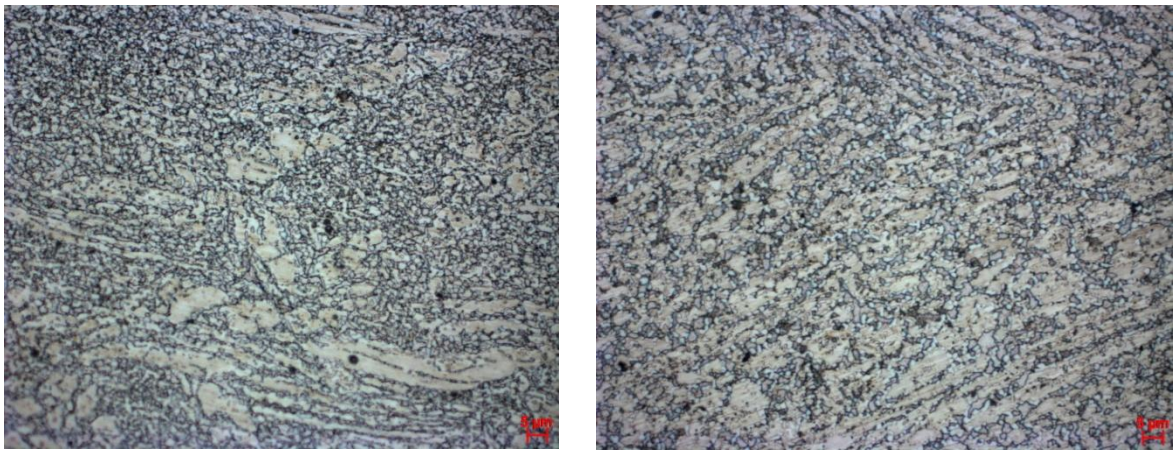

(a) **(b)**

Fig. 30: Optical microstructures after rolling of (a) Water Quenched,(b) Air cooled

Optical microscopy analysis shows the two phase structure. After rolling, Fig 30 (a), shows the samples which were water-quenched, the optical shows that the austenite grains are present in the ferrite matrix, whereas in Fig 30 (b), which shows the microstructure of the alloyed 2205 DSS at air cooled condition, there is the formation of sigma phase along the ferrite and austenite grain boundaries. Due to the air-cooling at room temperature the detrimental phases like sigma and chi got sufficient time to nucleate and grow. This data is more clear by using Scanning Electron Microscpy(SEM) whose results are stated below

5.5 Scanning Electron Microscopy(SEM)

This was done to identify the grains of Ferrite and austenite in the microstructure which are verified through the XRD analysis.

The samples were hot forged and hot rolled and the rolled samples were quenched in water to avoid the formation of any intermetallic compound. Fig 31 shows the SEM analysis of rolled samples prepared from copper and tungsten alloyed 2205 duplex stainless steel clearly shows the two phase region. The matrix is of ferrite whereas the austenite grains are spread throughout the ferrite matrix. Fully dark and black spots observed in SEM analysis are the porosities which are left during casting.

The SEM analysis shows the microstructure containing bright matrix region of ferrite and the dark region is austenite.

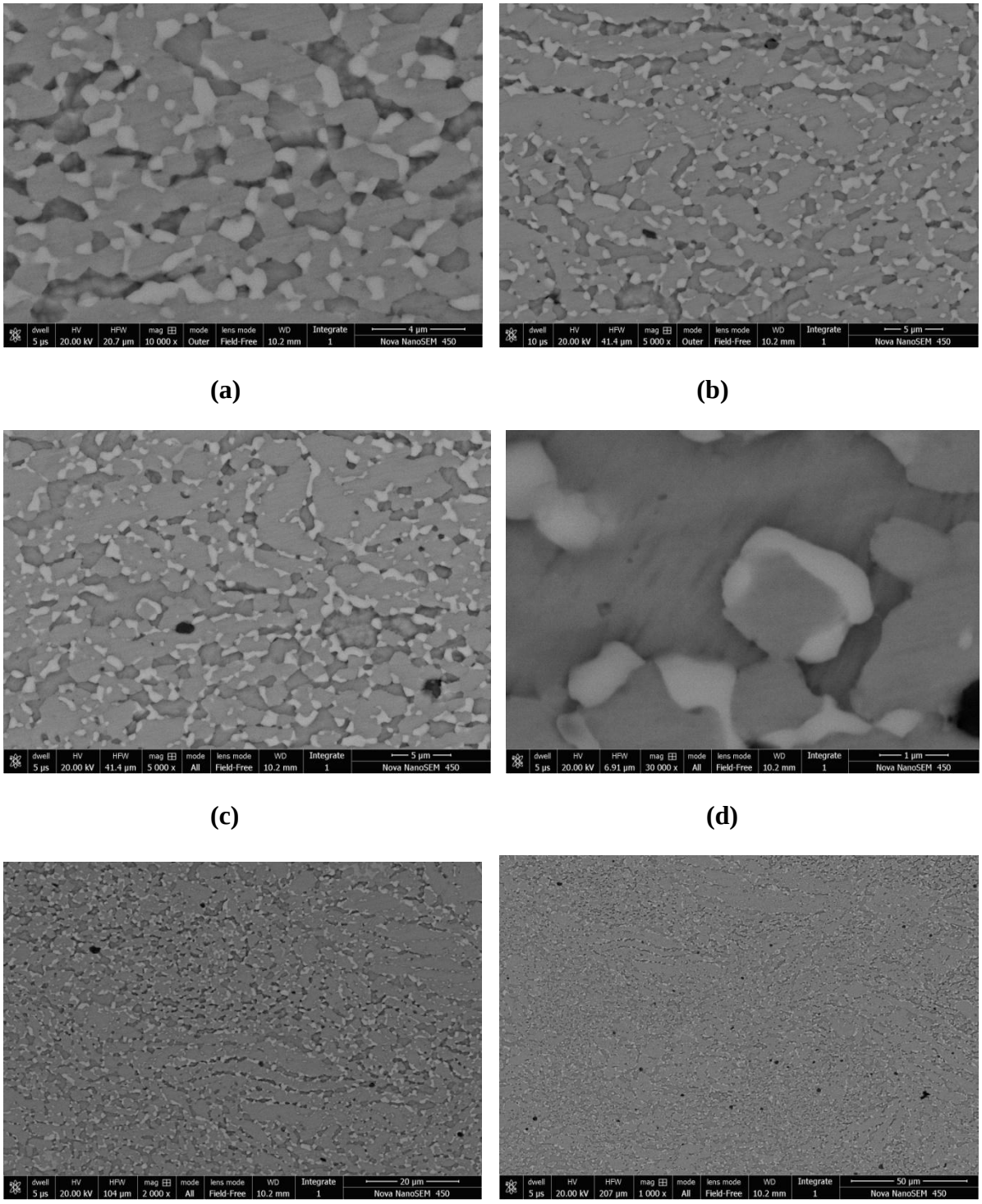

Fig. 31: Austenite grains in the ferrite matrix of the water quenched rolled samples of alloyed 2205 duplex stainless steel

These SEM analysis micrographs shown in Fig 32 are of alloyed 2205 duplex stainless steel in the air cooled state after rolling. Because of the air cooling after rolling, there micrographs are containing some amount of intermetallic phases. The phases that have precipitated are probably sigma and chi phase. As air cooling allows ample amount of time for the

precipitates to form and the tendency of formation of intermetallic compounds totally depends on the time and temperature. As discussed earlier the formation of precipitates depend on driven by particular temperature ranges.

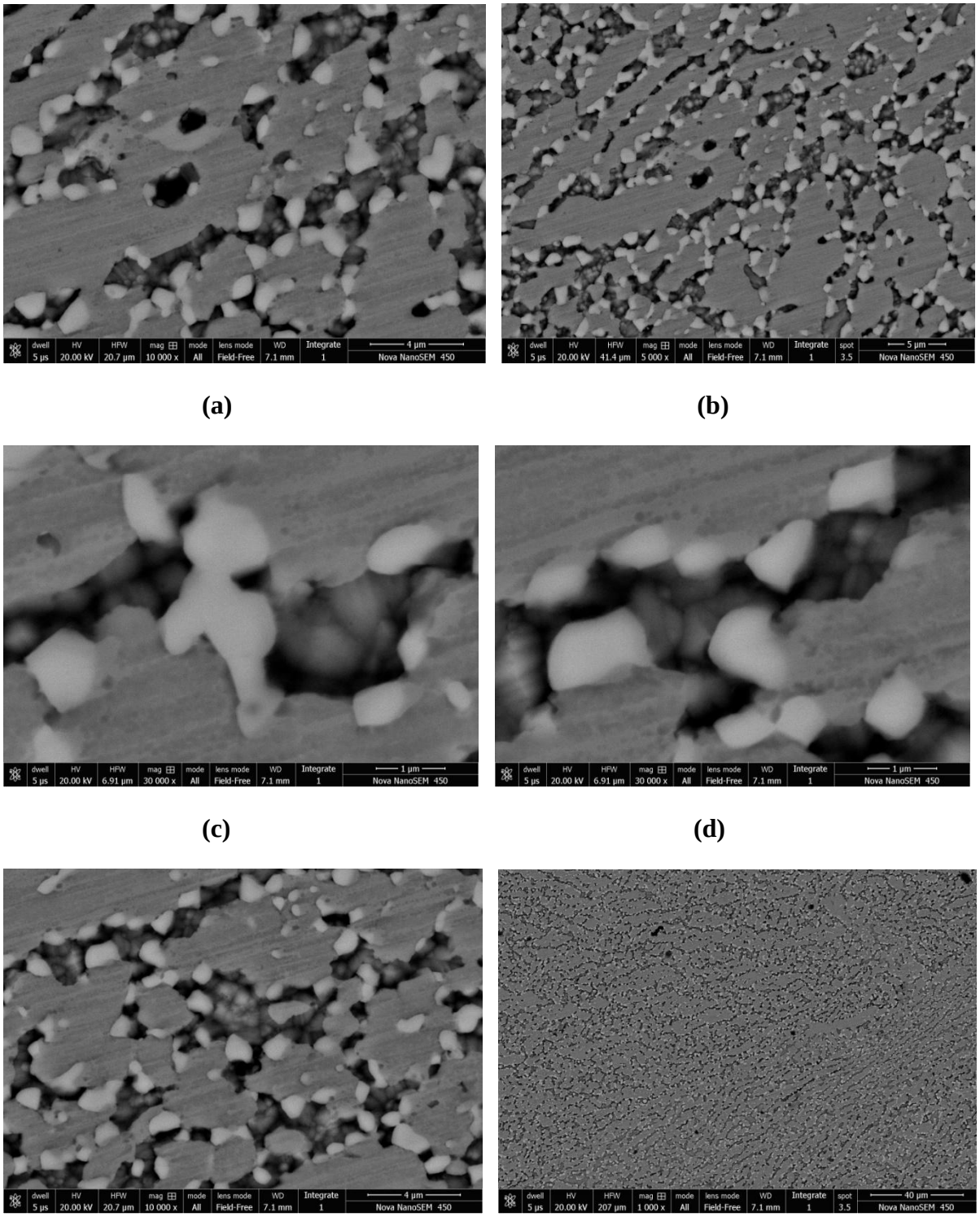

Fig. 32: Austenite grains in the ferrite matrix with some precipitates in the air cooled rolled samples of alloyed 2205 duplex stainless steel

5.6 DSC(Differential Scanning Calorimetry)

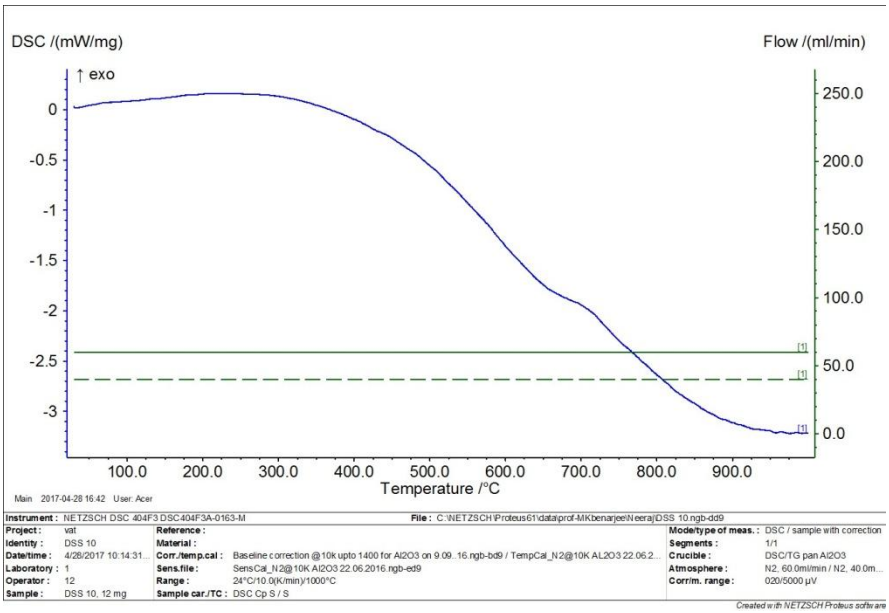

(a)

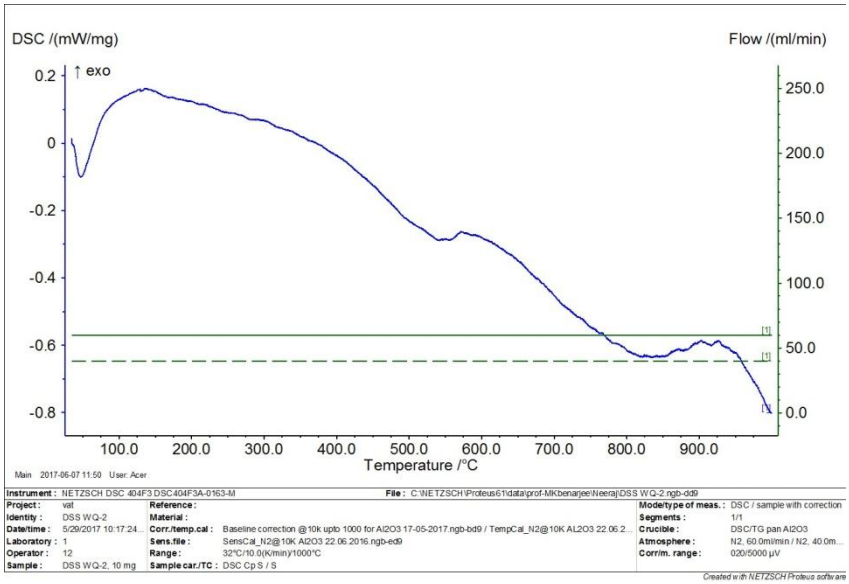

(b)

Fig. 33: DSC curve shows two endothermic peaks at around 650°C and 850°C

The differential scanning calorimetry analysis was performed on the water quenched Cu and W alloyed 2205 duplex stainless steel. Fig 33(a) shows the DSC curve when the samples was taken in the form of powder. The powder was obtained by rubbing the rolled sample on the filer and Fig 33(b) shows the DSC curve when the sample was taken in the form of solid the 10 mg sample in the solid form was obtained by shaper tool in the mechanical workshop

laboratory in our department. A partial endothermic peak was also observed at 300°C due to the formation of partial copper precipitates and alpha prime phase.

The conclusions drawn from the DSC curves show that three endothermic peaks were observed around temperature range of 300°C, 600-650°C and the other peak at 800-850°C.

Hence, the ageing behaviour was studied at these temperatures ranges in the later part of the project.

5.7 Hardness

Hardness study of samples prepared by solutionizing at 950°C and then ageing at different temperatures for 1 hour**.**

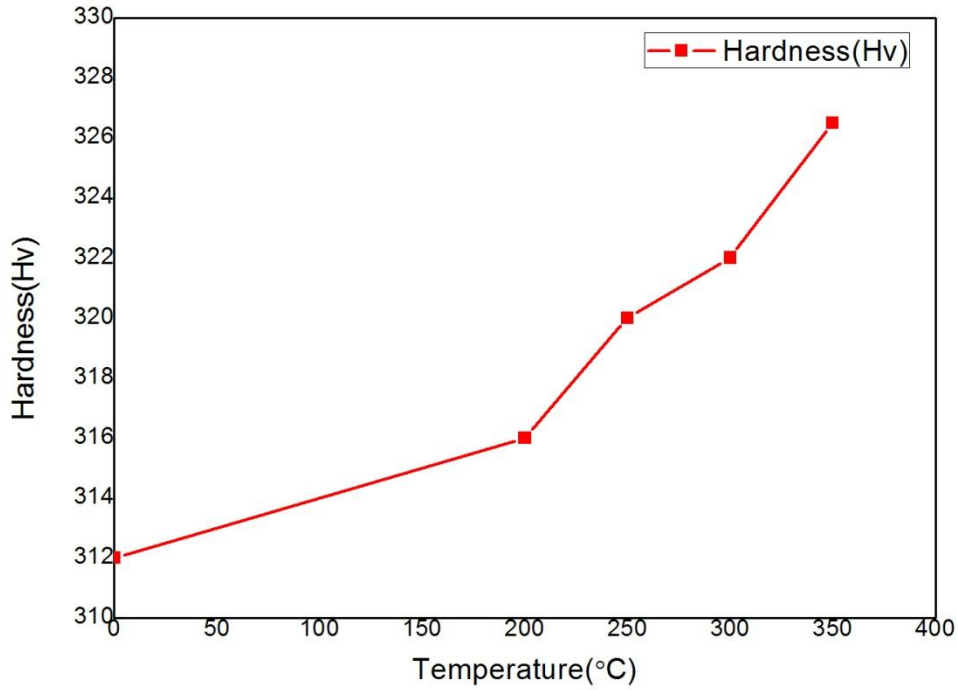

Fig. 34: Small increase in the hardness values with respect to temperature

Although there is no significant increase in the hardness values with respect to temperature But there is continuous increase in the hardness values which shows that there may be partial precipitation of copper in the alloy 2205 stainless steel. As any other intermetallic phase do not precipitate in such low temperature ranges after ageing for 1 hour, it confirms that there is partial copper precipitation in the matrix.

5.8 Hardness and SEM results of samples aged for different time intervals and different temperatures

5.8.1 Hardness study of samples prepared at solutionizing at 1150°C and then ageing at 300°C temperature and different ageing time

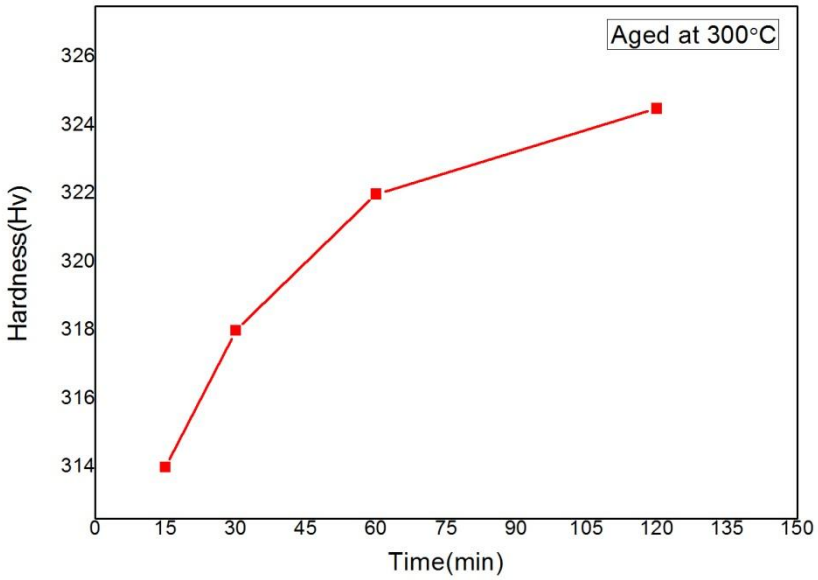

Fig. 35: Hardness values after ageing at 300°C with varying time interval

Four samples were prepared and solutionized at 1150°C and then quenching was done in ice-water. So that the formation of any intermetallic phase is minimised. Now ageing is done at 300°C with varying time at 15min, 30min, 60min, 120 min. The hardness graph shows a continuous increase in the hardness values with increase in ageing time at 300°C.

5.8.2 SEM analysis of samples aged at 300°C for 15 min are shown below

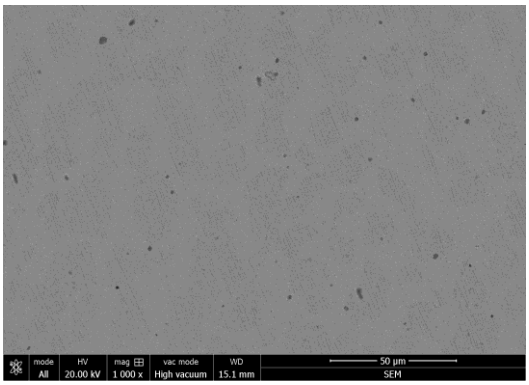

(a)

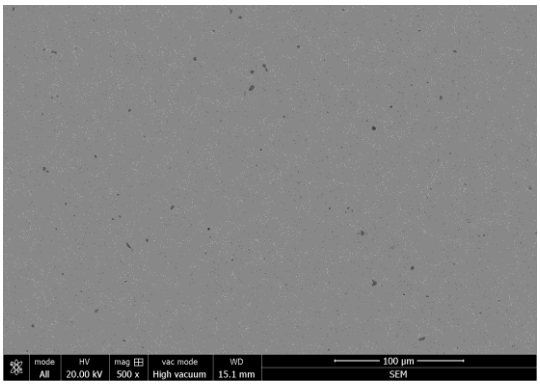

(b)

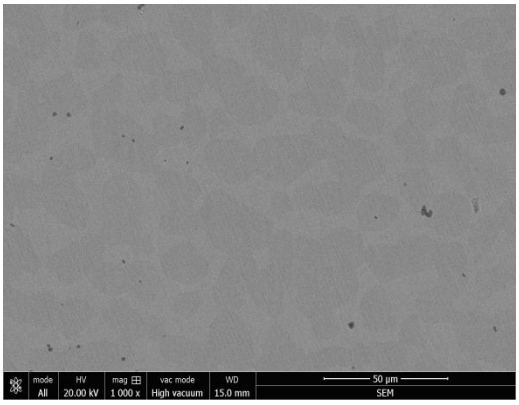

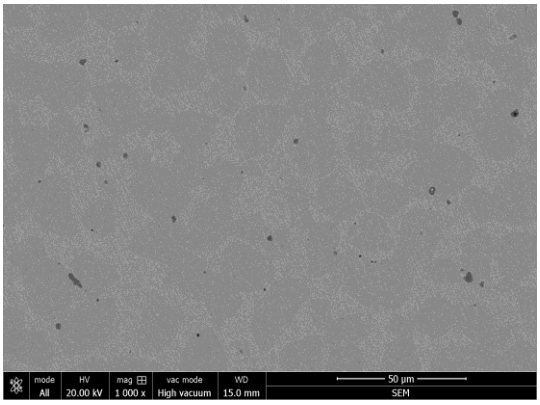

(c) **(d)**

Fig. 36: (a), (b), (c), (d) SEM graphs aged at 300°C for 15 minutes

These SEM micrographs shown in fig 36, have no significant amount of precipitation of any intermetallic or any copper precipitates. The micrographs just contain ferrite and austenite grains. The micrographs also show small amount of black porosities throughout the matrix.

Hence, there is no significant increase in hardness value when compared with the initial hardness i.e. at the rolled state.

5.8.3 SEM analysis of samples aged at 300°C for 30 min are shown below

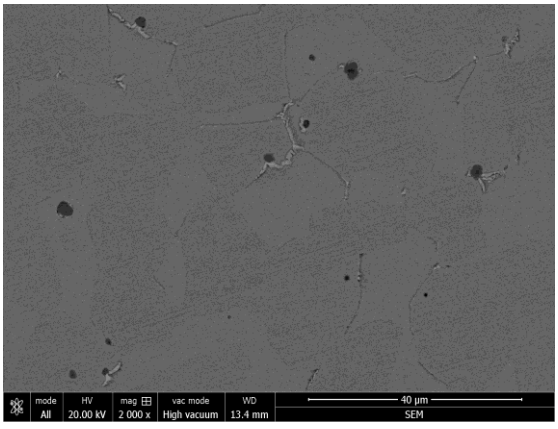

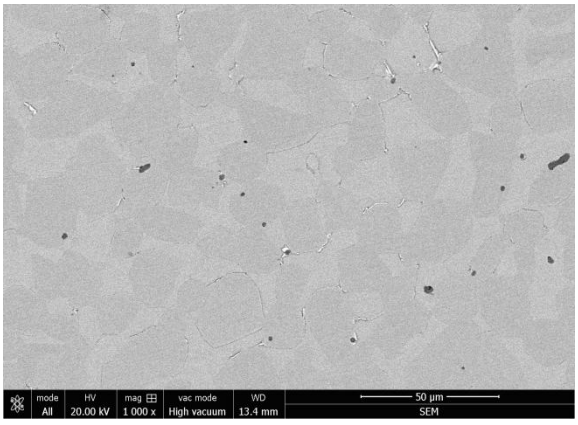

(a) **(b)**

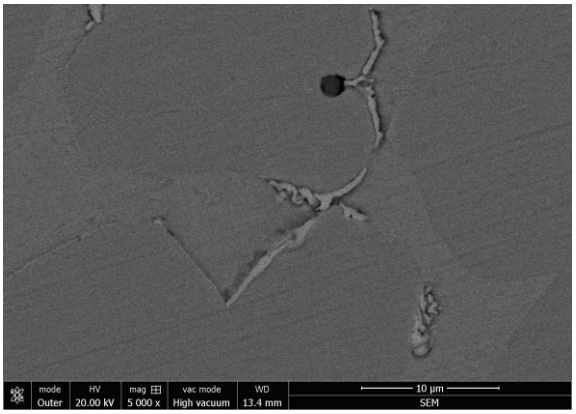

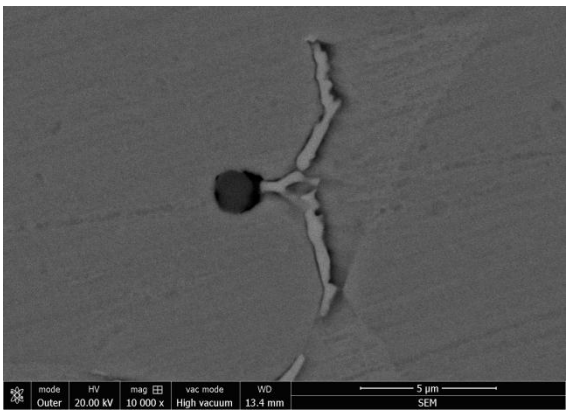

(c) **(d)**

Fig. 37: (a), (b), (c), (d) SEM graphs aged at 300°C for 30 minutes

These SEM micrographs shown in Fig 37, there might have been precipitation of copper and alpha prime phase. The formation of copper precipitation is not proper because of large amount of ferrite. Copper precipitation is observed at ferrite-ferrite grain boundaries and no precipitation or very few precipitates at ferrite-austenite or austenite-austenite grain boundaries. As proper copper precipitation has not occurred and hence the hardness of the sample has not increased significantly. Copper in austenite grains is either in the solution or there may be partial precipitation at grains or grain boundaries. The micrographs also show small amount of black porosities throughout the matrix.

Hence, there is partial increase in hardness value, when compared with the hardness at 300°C for 15 minutes.

5.8.4 SEM analysis of samples aged at 300°C for 60 min are shown below

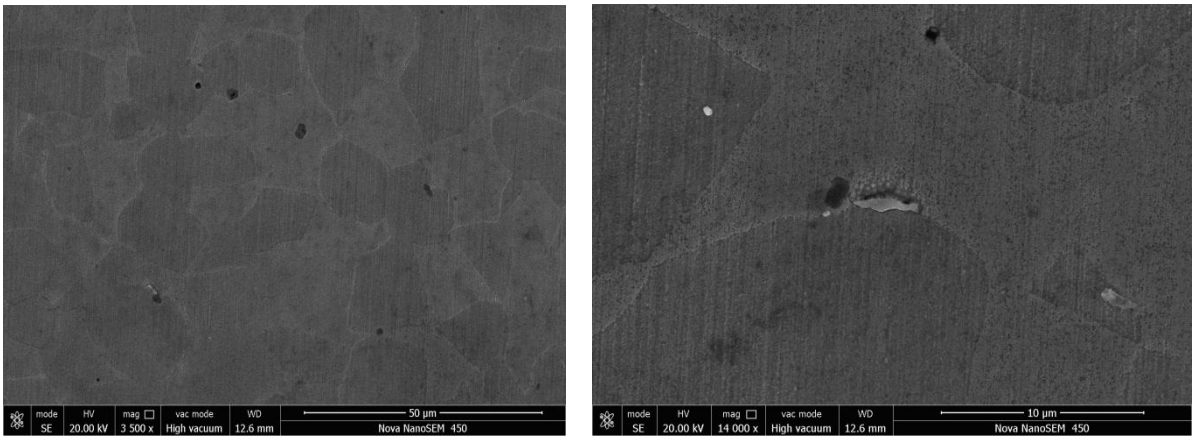

(a) **(b)**

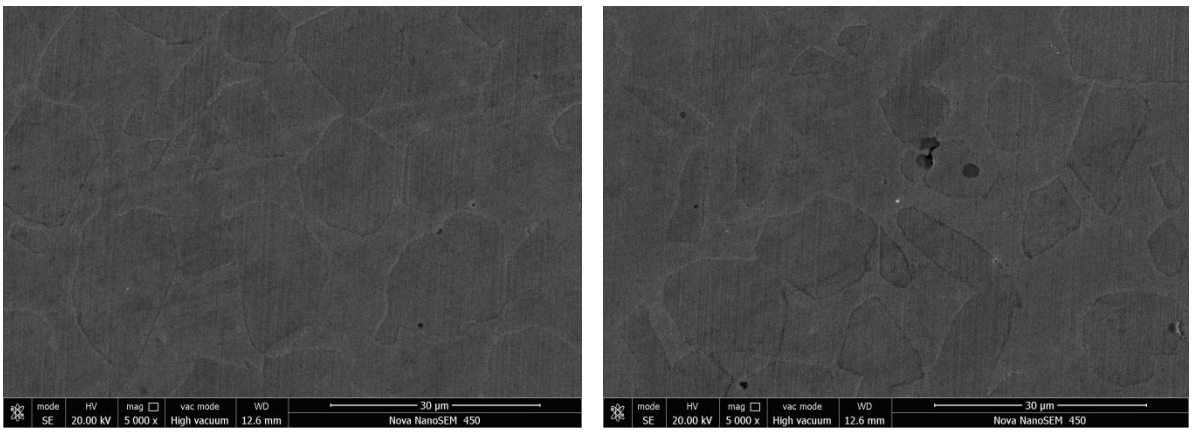

(c) **(d)**

Fig. 38: (a), (b), (c), (d) SEM graphs aged at 300°C for 60 minutes

These SEM micrographs shown in fig 38, there has been precipitation of copper and alpha prime phase. The formation of copper precipitation is now along all the grains boundaries. In this case also proper precipitation of copper has not been observed. This will also not result in any significant increase in hardness value. Copper has now precipitated at austenite grain boundaries. The micrographs also show small amount of black porosities throughout the matrix.

Hence, there is increase in hardness value, when compared with the hardness at 300°C for 15 minutes and 30 minutes.

5.8.5 SEM analysis of samples aged at 300°C for 120 min are shown below

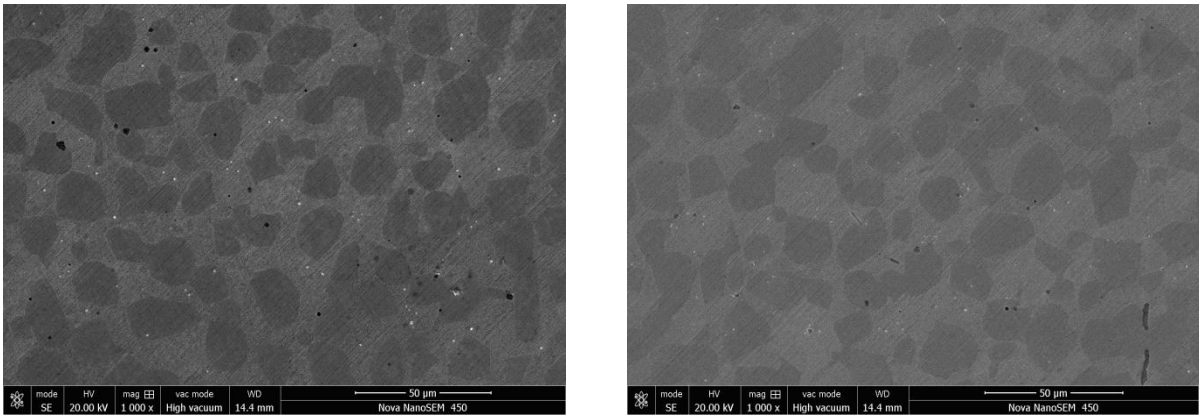

(a) **(b)**

Fig. 39: (a), (b) SEM graphs aged at 300°C for 120 minutes

These SEM micrographs shown in fig 39, there has been precipitation of copper and alpha prime phase. The formation of copper precipitation is now along all the grains boundaries. In this case also proper precipitation of copper has not been observed. This will also not result in any significant increase in hardness value. Although the hardness value is increasing that refects the fact that there is increase in precipitation behaviour. The micrographs also show small amount of black porosities throughout the matrix.

5.8.6 Hardness study of samples prepared at solutionizing at 1150°C and then ageing at 650°C temperature and different ageing time

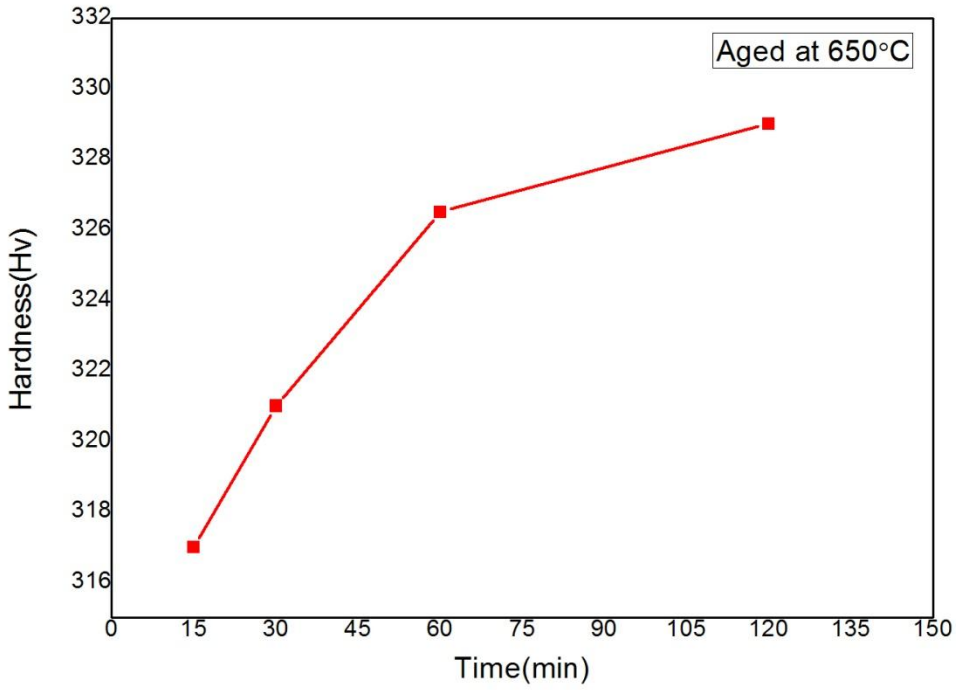

Fig. 40: Hardness values after ageing at 650°C with varying time interval

Four samples were prepared and solutionized at 1150°C and then quenching was done in ice-water. So that the formation of any intermetallic phase is minimised. Now ageing is done at 650°C with varying time at 15min, 30min, 60min, 120 min. The hardness graph shows a continuous increase in the hardness values with increase in ageing time at 650°C.

5.8.7 SEM analysis of samples aged at 650°C for 15 min are shown below

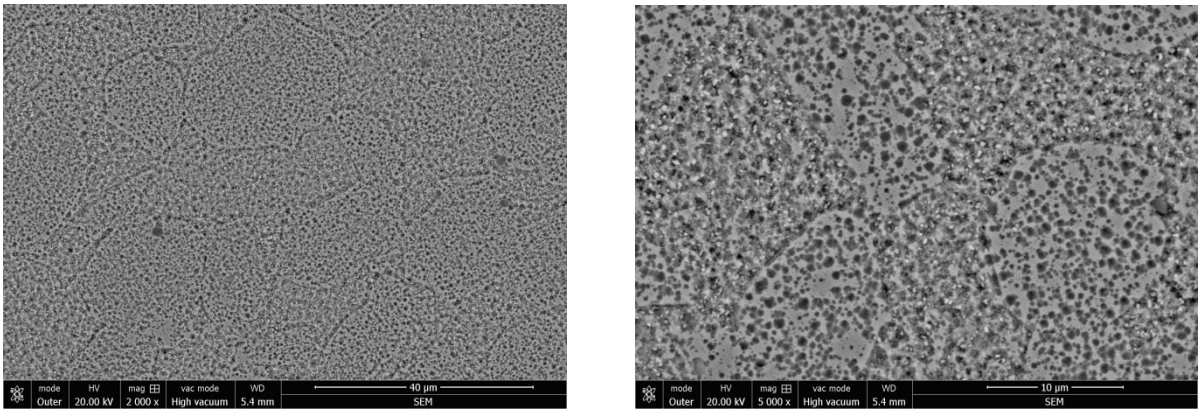

(a) **(b)**

Fig. 41: (a), (b) SEM graphs aged at 650°C for 15 minutes

These SEM micrographs shown in fig 41, there has been excessive pitting due to the use of etchant for long time. The etchant contains large amount of chloride ions which has resulted

in severe pitting to occur throughout the sample. Because of this excessive pitting Molybdenum-rich chi phase has precipitated along with sigma phase. The precipitation of chi phase is clearly observed around the grain boundaries. Sigma phase precipitation is not clear due to the pitting that has occurred throughout the sample.

5.8.8 SEM analysis of samples aged at 650°C for 30 min are shown below

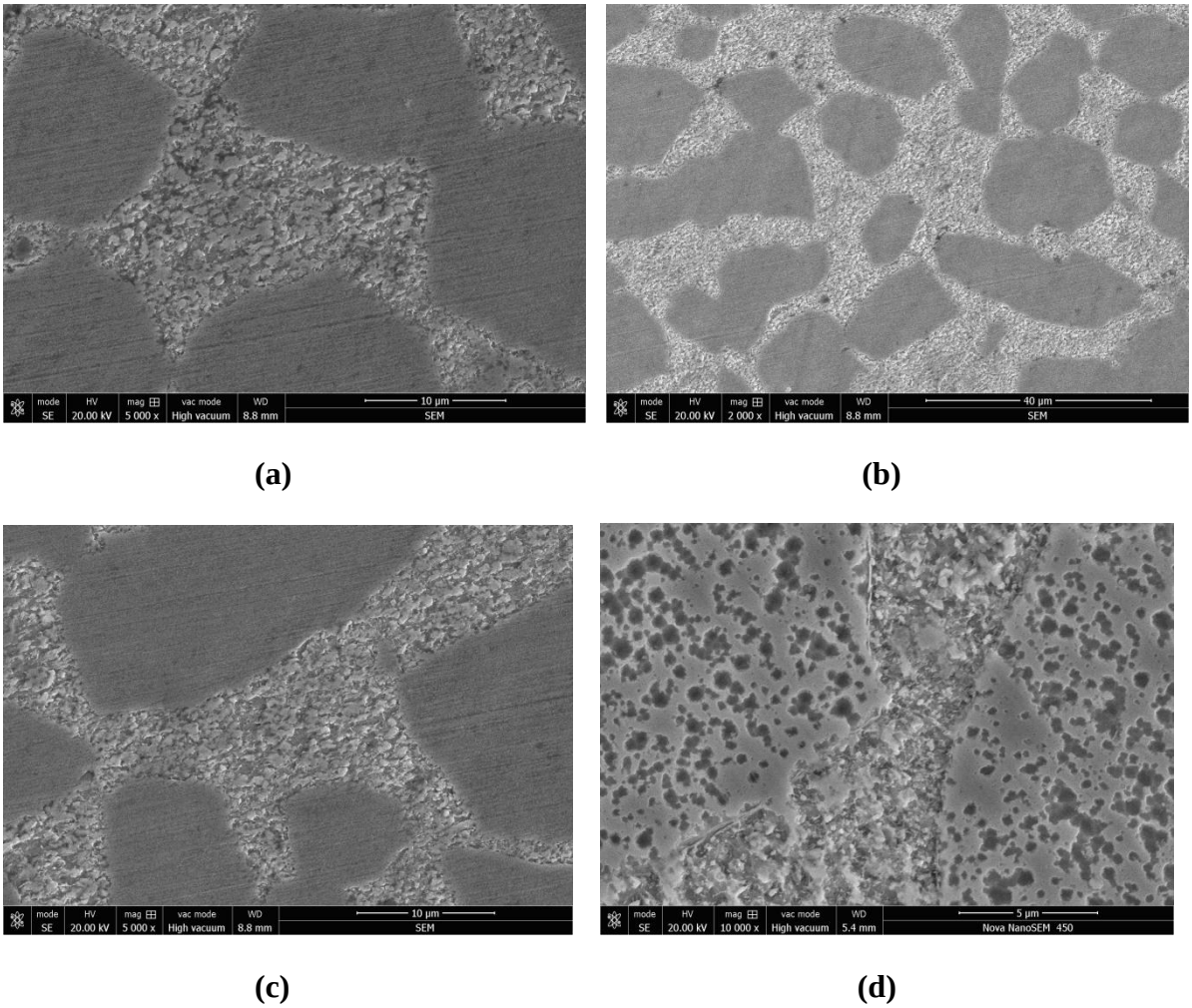

(a) **(b)**

(c) **(d)**

Fig. 42: (a), (b), (c), (d) SEM graphs aged at 650°C for 30 minutes

SEM micrographs shown in fig 42, also show the presence of chi as well as sigma phase. The formation of sigma phase occurs through the typical eutectoid reaction in ferrite matrix.

$$\alpha \longrightarrow \gamma_2 + \sigma$$

Hence, there is some formation of secondary austenite phase along with sigma phase. The intermetallic phases like sigma phase, chi phase and secondary austenite are precipitated in the ferrite matrix. Fig 42 (d), again shows the pitting formation due to excessive chloride etching.

5.8.9 SEM analysis of samples aged at 650°C for 60 min are shown below

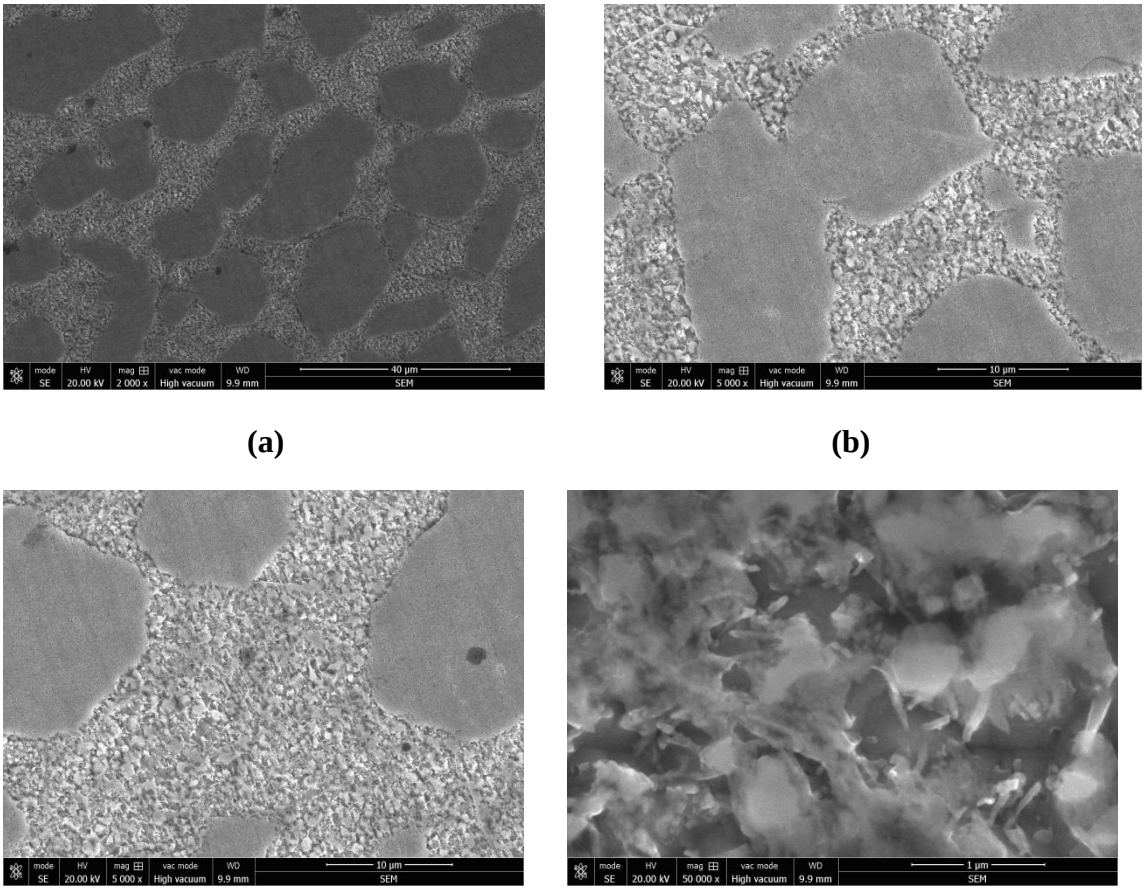

Fig. 43: (a), (b), (c), (d) SEM graphs aged at 650°C for 60 minutes

SEM micrographs shown in fig 43, also show the presence various intermetallic phases like sigma phase, chi phase, secondary austenite. The formation of sigma phase occurs through the typical eutectoid reaction in ferrite matrix.

$$\alpha \longrightarrow \gamma_2 + \sigma$$

Hence, there is some formation of secondary austenite phase along with sigma phase. Most of thses phases are precipitated along the ferrite matrix. The amount of precipitation or say precipitated phases has increased with increase in ageing time from 30min to 60 min at 650°C.

5.8.10 SEM analysis of samples aged at 650°C for 120 min are shown below

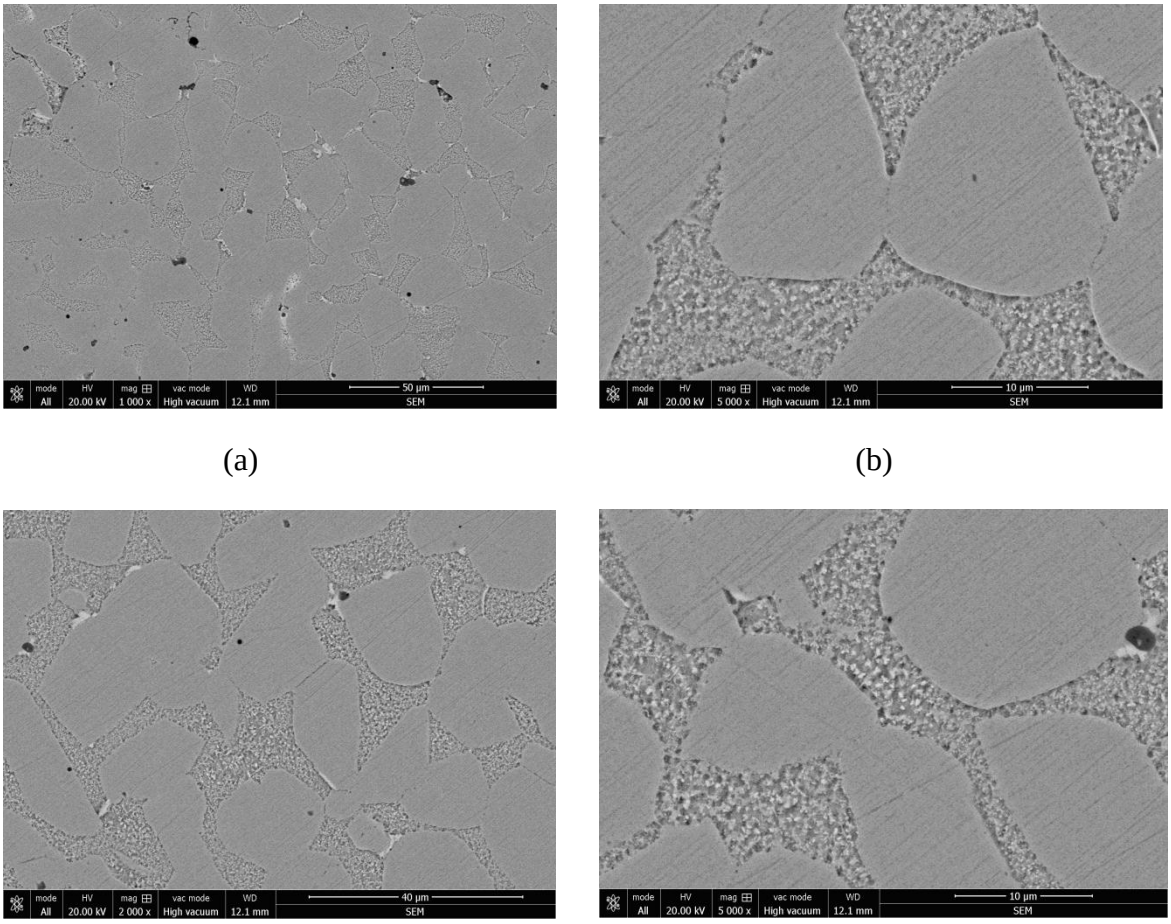

Fig. 44: (a), (b), (c), (d) SEM graphs aged at 650°C for 120 minutes

SEM micrographs in Fig 44, again show the same intermetallic precipitates as in above cases i.e. sigma, chi and secondary austenite phases. The only difference is the amount of precipitates which is maximum in this case. As the presence of intermetallic phases increases with increase in ageing time, this also justifies why there is continuous increase in hardening behaviour with increase in ageing time.

5.8.11 Hardness study of samples prepared at solutionizing at 1150°C and then ageing at 850°C temperature and different ageing time

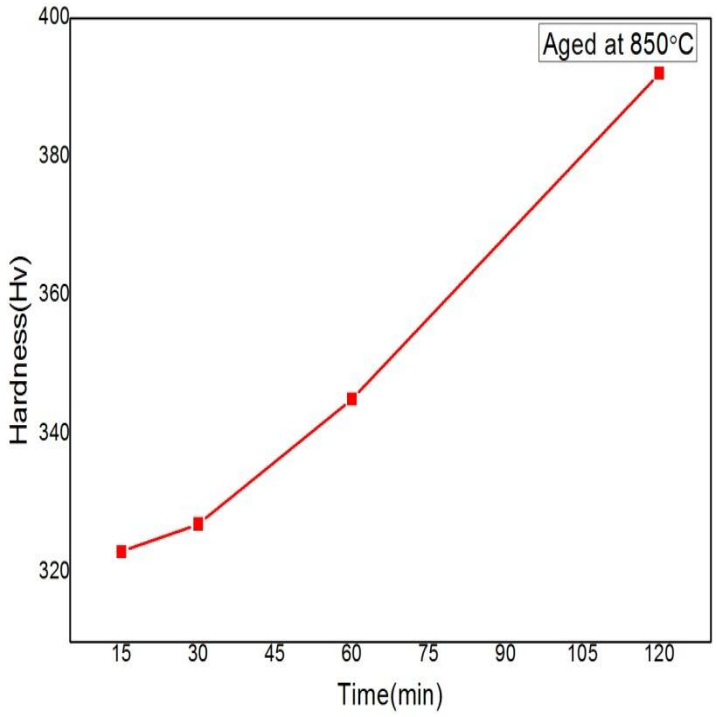

Fig. 45: Hardness values after ageing at 850°C with varying time interval

Four samples were prepared and solutionized at 1150°C and then quenching was done in ice-water. So that the formation of any intermetallic phase is minimised. Now ageing is done at 850°C with varying time at 15min, 30min, 60min, 120 min. The hardness graph shows a continuous increase in the hardness values with increase in ageing time at 850°C.

After the increase in ageing time from 30min to 60 min and from 60 min to 120 min there has been sudden increase in the hardness values this is because of the fact that there has been excessive formation of sigma and chi phases as these phases are best precipitated in this temperature range. The precipitation of tungsten carbide also occurs in this temperature. This also contributes to sudden increase in hardness values. These results are also cross verified through the SEM analysis.

5.8.12 SEM analysis of samples aged at 850°C for 15 min are shown below

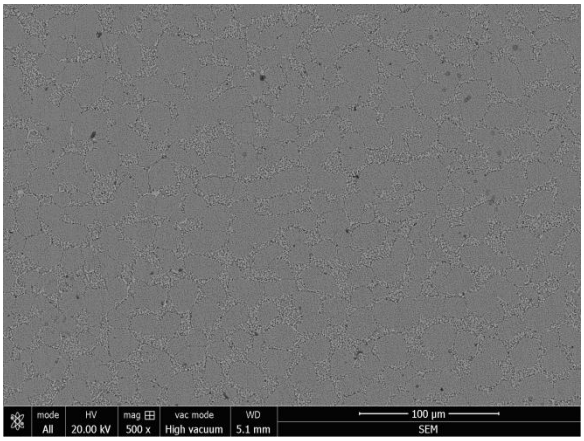

(a)

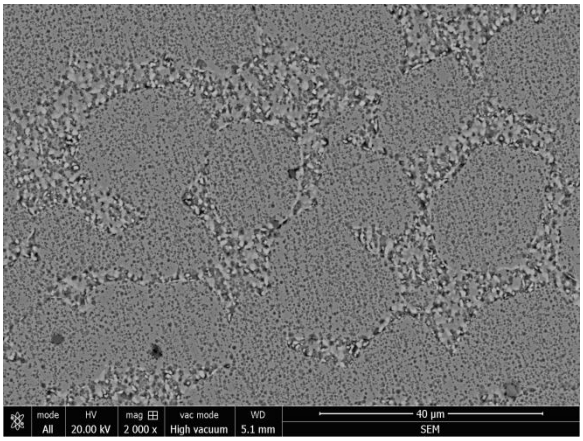

(b)

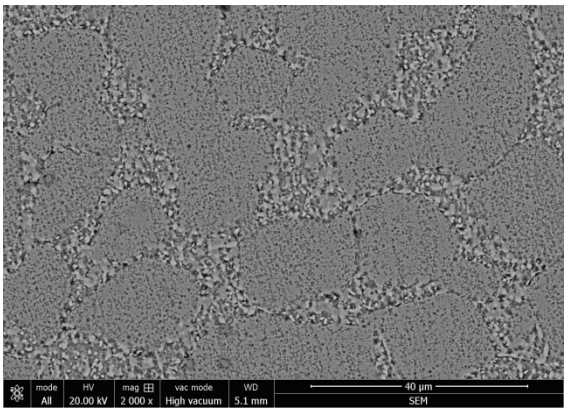

(c)

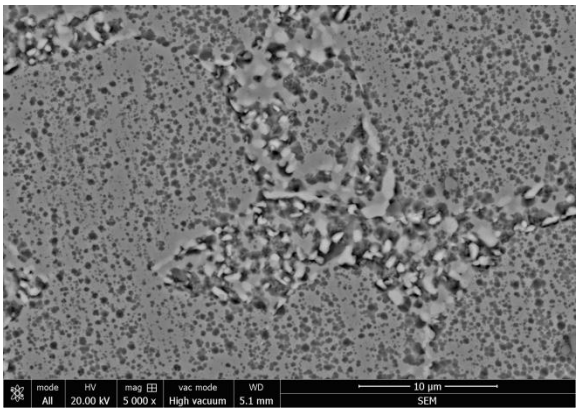

(d)

Fig. 46: (a), (b), (c), (d) SEM graphs aged at 850°C for 15 minutes

SEM micrographs in Fig 46, shows massive formation of intermetallic phases even after 15 min of ageing at 850°C. Sigma phase has precipitated at the ferrite grains using a eutectoid reaction. Chi phase precipitate at the ferrite grain boundaries. Formation of tungsten carbide also occurs in this high ageing temperature. Presence of pitting is observed on the austenite phase. Pitting has occurred because of etchant used is rich in chloride ions. As the molybdenum-rich phases dominate the ferrite phases and hence the regions of autenite have become Mo-deficient and hence pitting is more dominant at austenite grains.

5.8.13 SEM analysis of samples aged at 850°C for 30 min are shown below

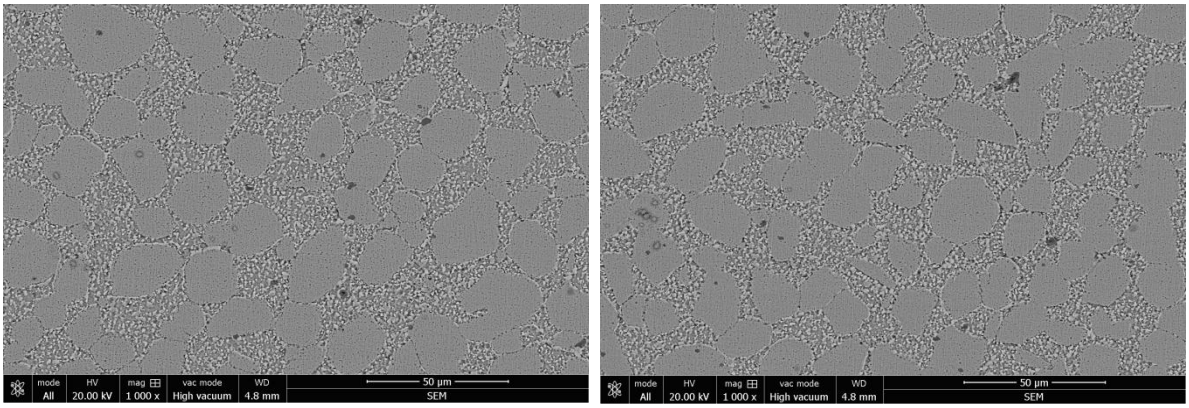

(a) **(b)**

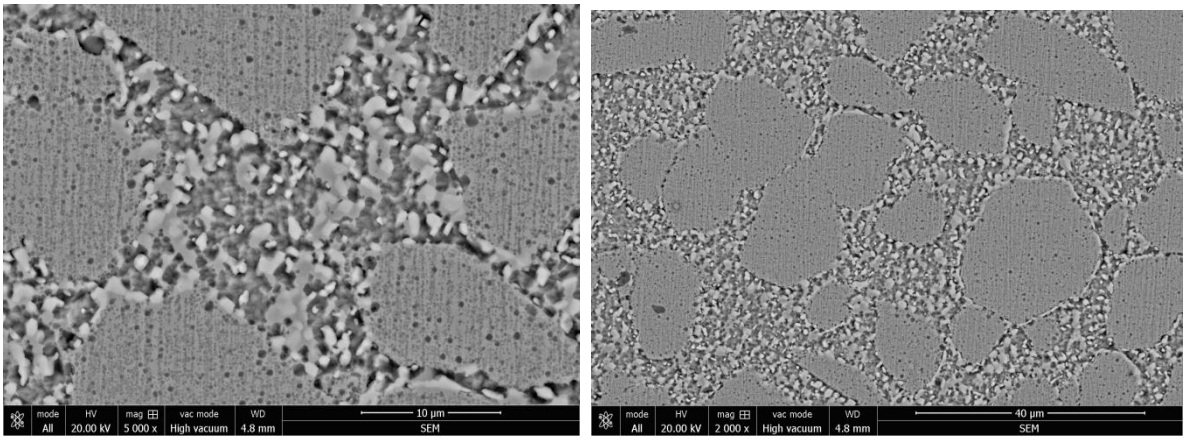

(c) **(d)**

Fig. 47: (a), (b), (c), (d) SEM graphs aged at 850°C for 30 minutes

SEM micrographs in Fig 47, show the formation of various intermetallic phases along with tungsten carbides. The amount of these phases increases with increase with aging time. Hence we can observe increase in hardness values because the amount of phases increase. These phases increase the hardness values of these steels. Pitting is also observed throughout the micrograph with domination in the austenite regions.

5.8.14 SEM analysis of samples aged at 850°C for 60 min are shown below

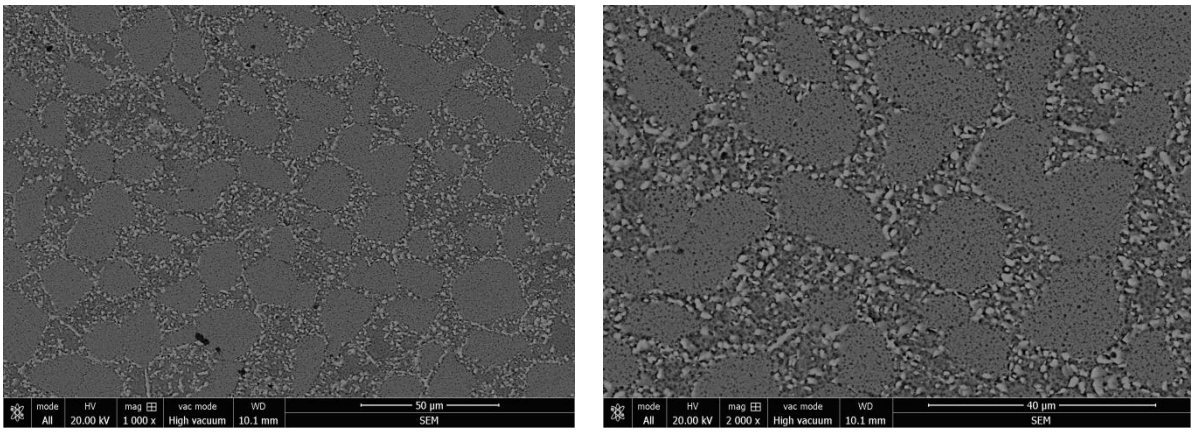

(a) **(b)**

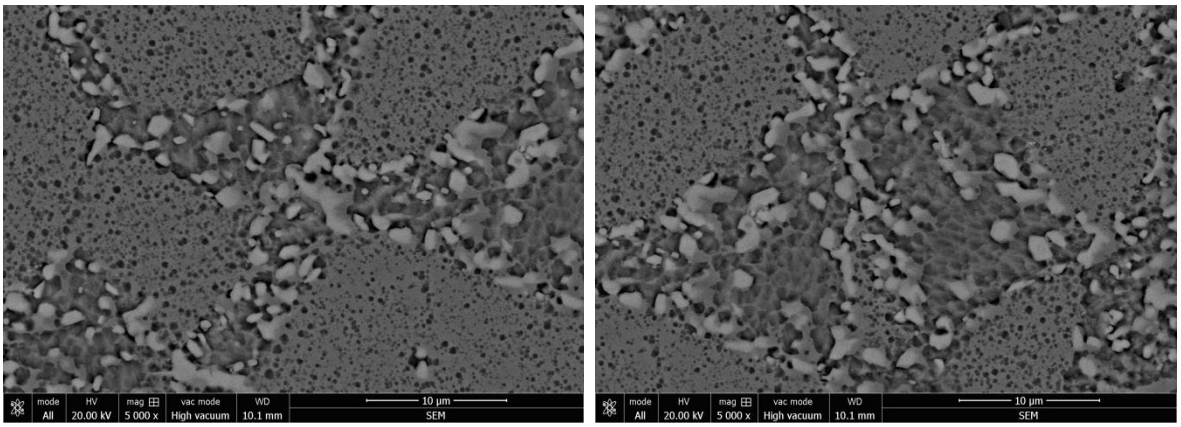

(c) **(d)**

Fig. 48: (a), (b), (c), (d) SEM graphs aged at 850°C for 60 minutes

SEM micrographs in Fig 48, again show the intermetallic and tungsten carbide precipitates but this time the amount of these precipitates is quite high and hence there is sudden increase in the hardness values. The tungsten carbide precipitates have also increased and hence hardness values are also increased as shown in the hardness curve. The formation is also severe and is clearly seen throughout the micrograph.

5.8.15 SEM analysis of samples aged at 850°C for 120 min are shown below

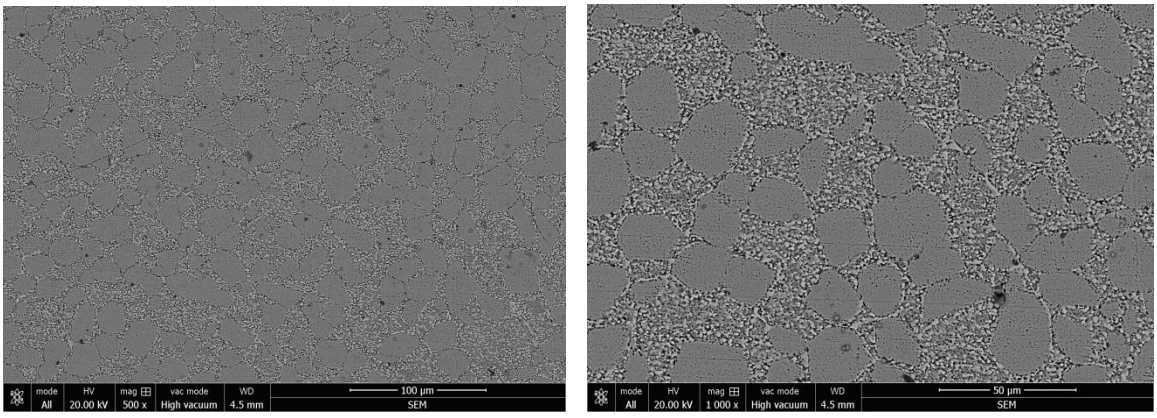

(a) **(b)**

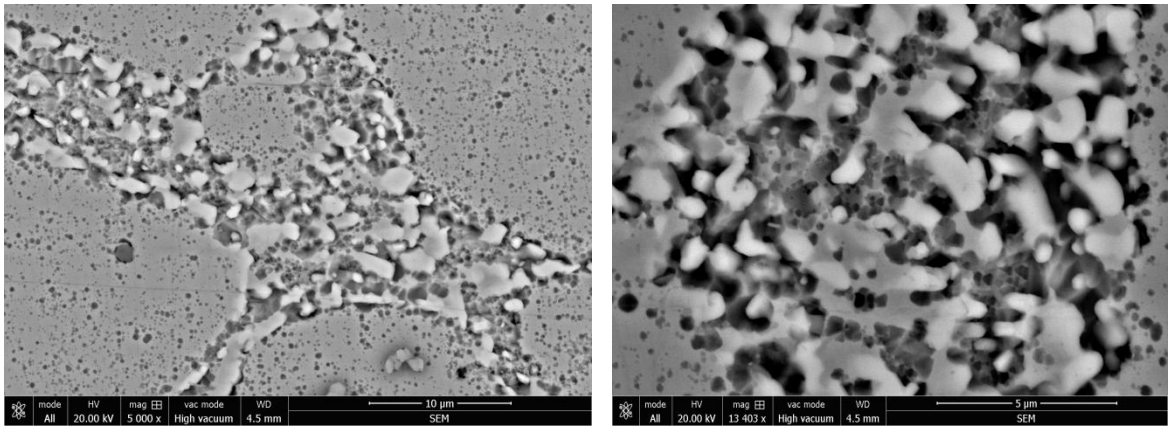

(c) **(d)**

Fig. 49: (a), (b), (c), (d) SEM graphs aged at 850°C for 120 minutes

SEM micrographs in Fig 49, shows the intermetallic and tungsten carbide precipitates as in the previous few cases the only difference is the amount of these precipitates which is quite high and hence there is sudden increase in the hardness values. The amount of tungsten carbides might also have been increases one of a sudden which also might be the factor for sudden increase in the hardness values as shown in the hardness curve. The formation is also severe and is clearly seen throughout the micrograph.

5.9 Gleeble

Hot compression test was performed on the copper and tungsten alloyed 2205 duplex stainless steel. The strain rate and temperature were selected as the variables. Strain rate 1, 10, 20 were selected and temperature of 900°C, 1000°C, 1100°C.

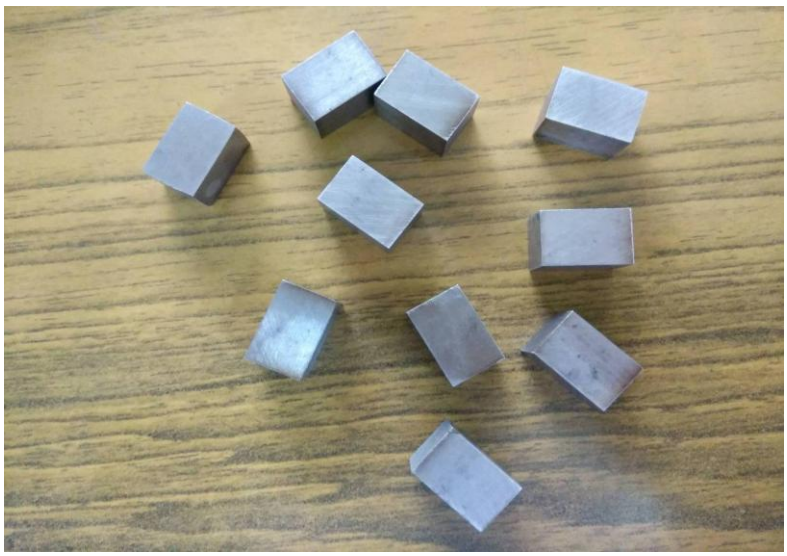

Fig. 50: Samples prepared for hot compression in Gleeble 3800

(a) **(b)**

Fig. 51: (a), (b) shows the samples after hot compression

Controlled thermo-mechanical simulation was performed in the Gleeble 3800 simulator. The hot compression test was performed at high strain rates. Thermocouple is attached to the sample using a spot welder. Thermocouple is used to measure the temperature and also to control the temperature of the sample. The samples were heated at a rate of 5°C/sec and then held at a desired temperature for 30 seconds before compressing the sample at various strain rates. The samples were quenched quickly using a cooling system at the back of gleeble 3800.

5.9.1 Hot deformation at strain rate 1 and temperature variation

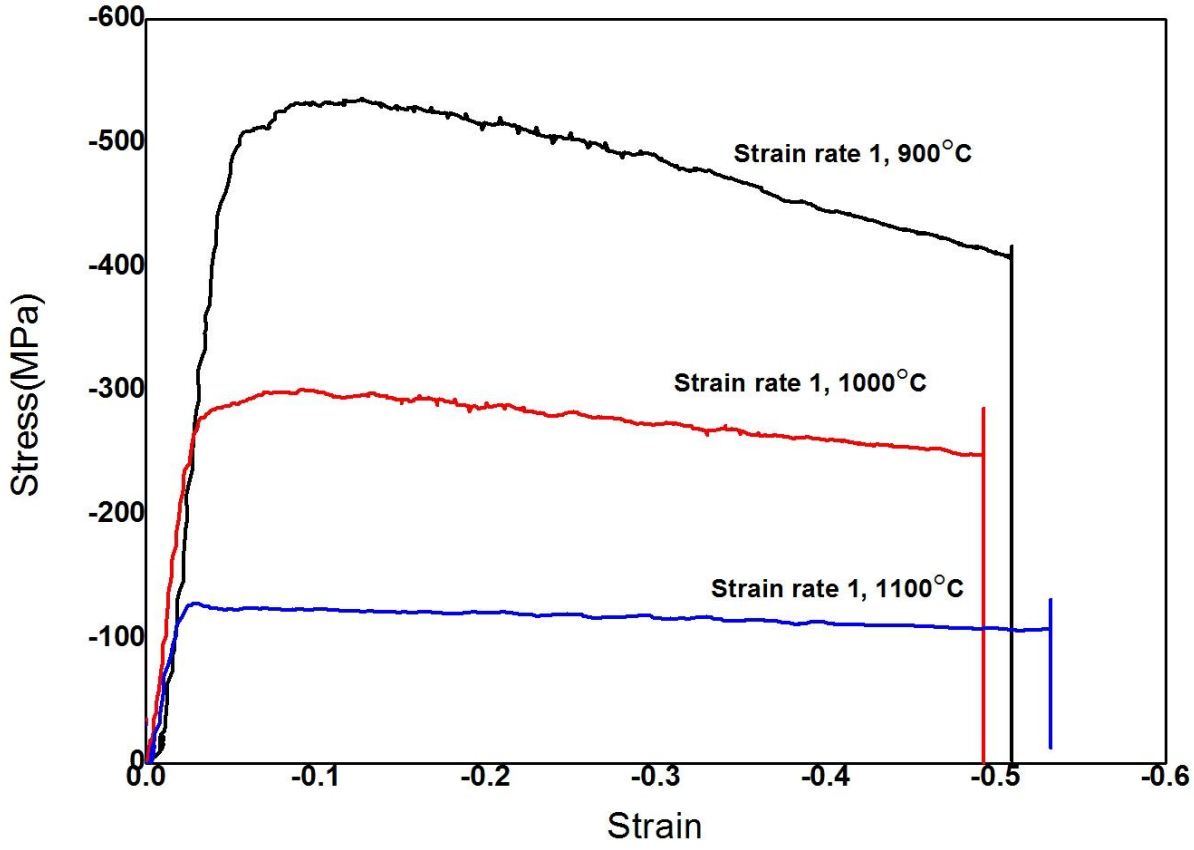

Fig. 52: True stress vs true strain curve at strain rate 1 & temperature 900°C, 1000°C, 1100°C

In Fig 52, Hot compression test at strain rate 1 and temperature 1100°C shows Dynamic recrystallization behaviour (DRX). At 1100°C dynamic recrystallization mechanism is observed. At temperature 1000°C, only dynamic recovery(DRV) occurs and no DRX is observed during hot compression. At 900°C, continuous softening and dynamic recovery both the mechanism are identified. In this also no DRX is observed. At strain rate 1, there is no sign of strain hardening.

5.9.2 Hot deformation at strain rate 10 and temperature variation

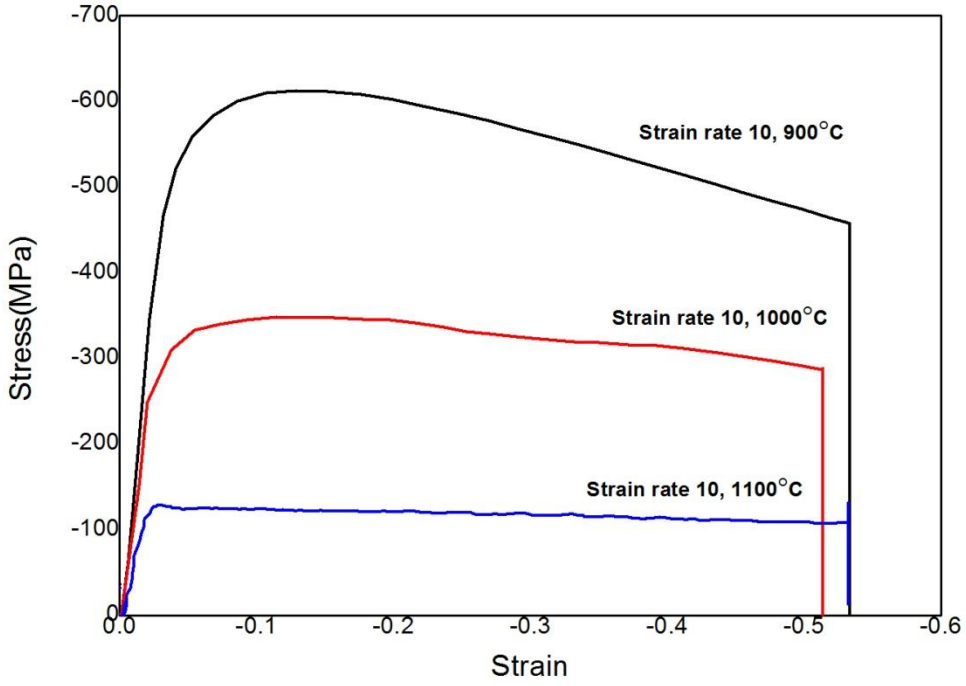

Fig. 53: True stress-true strain curve at strain rate 10 & temperature 900°C, 1000°C, 1100°C

Fig 53 shows, the similar pattern as shown at 1 strain rate is observed. At 1100°C the hot compression test shows DRX behaviour whereas at 1000°C, DRV is dominating the test and at 900°C, the test is dominate by both DRV and softening mechanism. No strain hardening occurs at this srtain rate.

5.9.3 Hot deformation at strain rate 20 and temperature variation

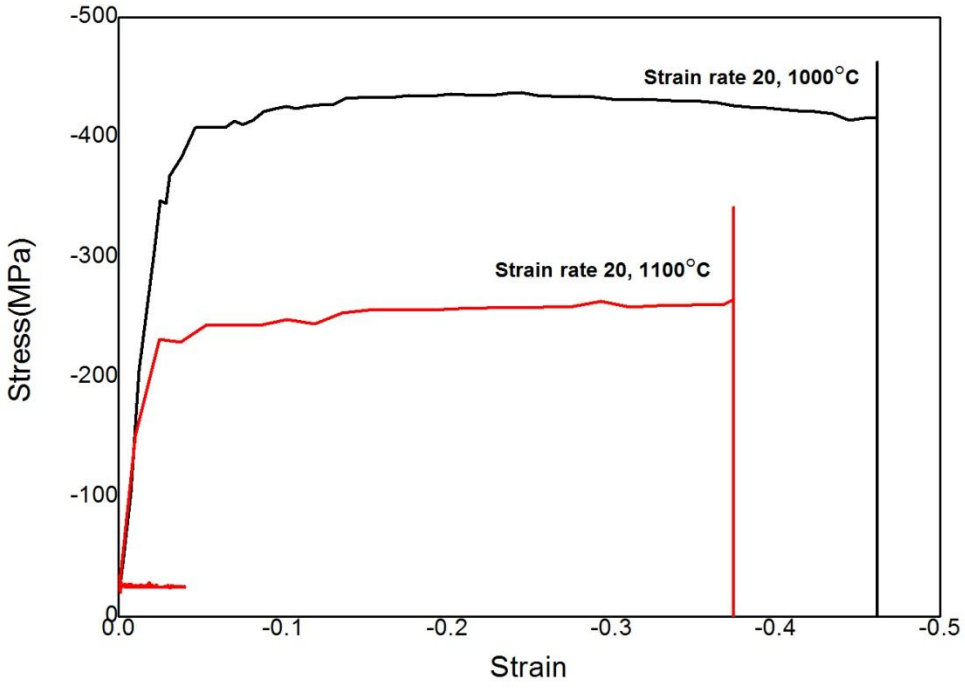

Fig. 54: True stress vs true strain curve at strain rate 20 & temperature 1000°C, 1100°C

At high strain rates no dynamic recrystallization (DRX) or dynamic recovery (DRV) behaviour or softening is observed instead there has been dynamic strain ageing and strain hardening mechanisms which are dominating the hot deformation tests.

DRX is only observed at 1100°C at strain rates 1 and 10. From the fig 52, 53 and 54 it is clear that the DRX behaviour is reducing with increase in strain rate from 1 to 20.

5.9.4 Hot deformation at 900°C and strain rates 1, 10

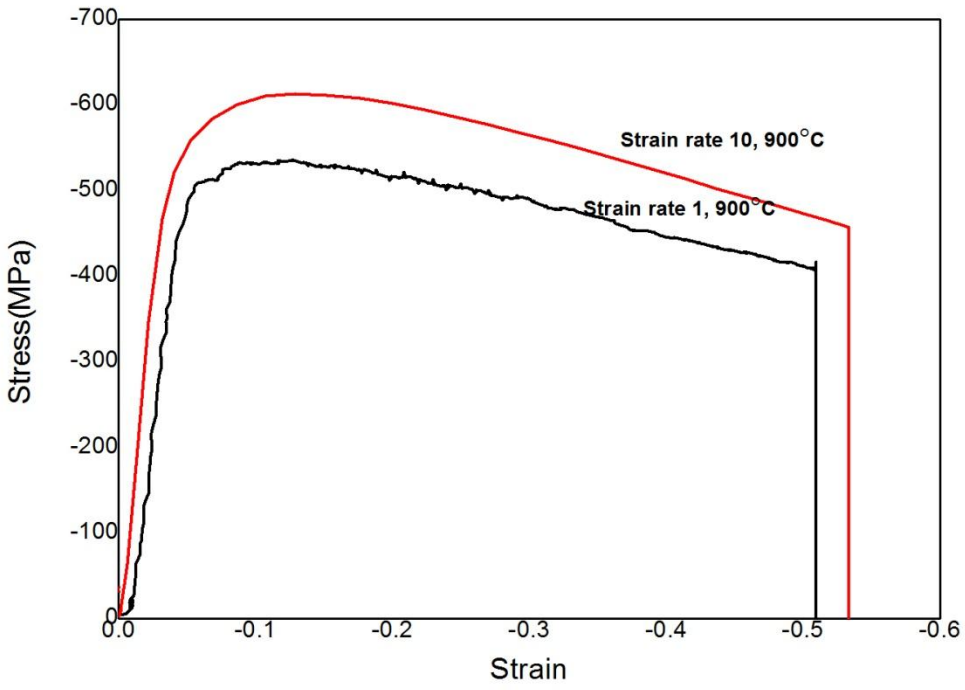

Fig. 55: True stress vs true strain curve at temperature 900°C and strain rate 1, 10

At same temperature 900°C and different strain rates the curve at strain rate 1 shows the serrations. These serrations are observed due to dynamic strain ageing behaviour. The phenomenon of serrations in stress strain curve due to dynamic strain ageing is well described by Portevin-Le Chatelier effect. No serrations were observed at 10 strain rate at same temperature. No DRX is observed at 900°C by varying strain rates.

5.9.5 Hot deformation at 1000°C and strain rates 1, 10 and 20

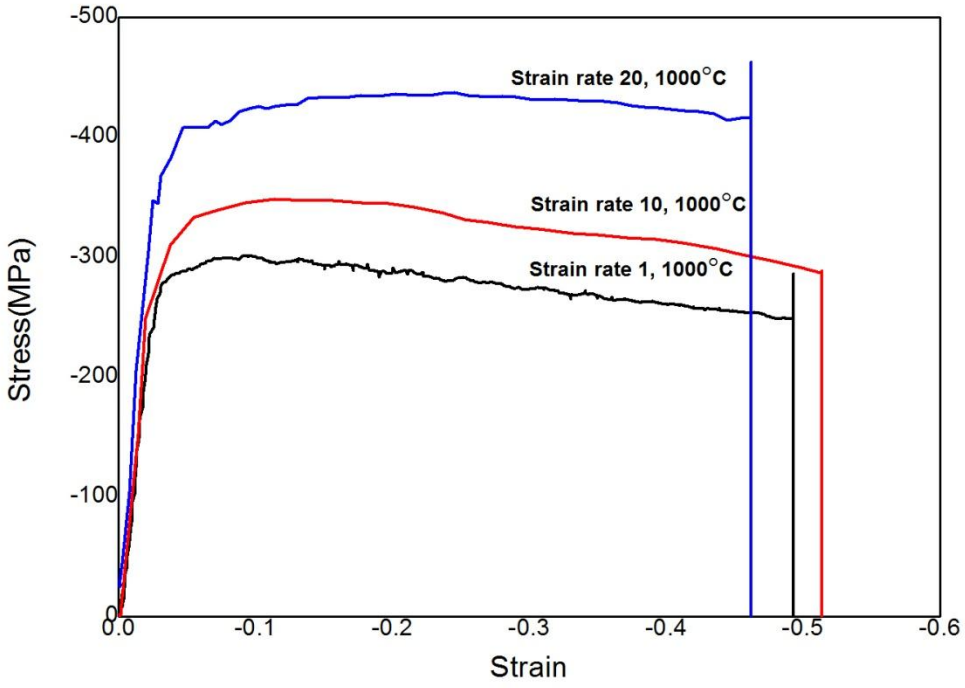

Fig. 56: True stress vs true strain curve at temperature 1000°C and strain rate 1, 10, 20

At constant temperature of 1000°C and strain rate 1 and 20 the serrations were observed throughout the compression test. No such serrations are observed at strain rate 10. The amplitude of serrations is increased at high strain rates because at high temperature flow stress decreases and the movement of solute particles is also high along with the dislocation movement which is also high. This results in either cutting or shearing mechanism for dynamic strain ageing. No DRX is observed at 1000°C at different strain rates.

5.9.6 Hot deformation at 1100°C and strain rates 1, 10 and 20

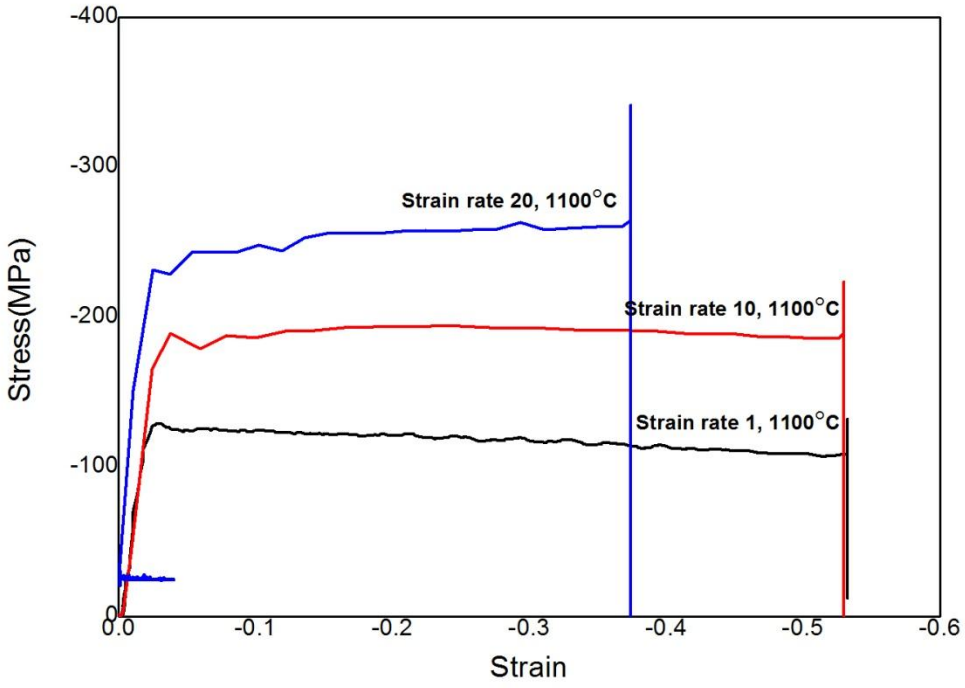

Fig. 57: True stress vs true strain curve at temperature 1100°C and strain rate 1, 10, 20

At constant temperature of 1100°C, at strain rate 1 the solute atoms lock the grains boundaries. Dynamic strain ageing behaviour is observed at strain rate 1. The movement of dislocations and the solute atoms is counter-balanced and hence the dynamic recovery (DRV) mechanism occurs at strain rate 10. At high strain rates i.e. 20, the dislocation cuts the solute atoms resulting in strain hardening. The serrations at strain rate 1 and 20 are observed because of this dynamic strain ageing behaviour. The dynamic strain ageing behaviour is due to either shearing of precipitate by dislocation or by cutting mechanism of the precipitate. The amplitude of serrations is increased at high strain rates, this is due to the velocity of dislocations and solute atoms increases as flow stress decreases at high temperature and this affects the dynamic strain ageing behaviour.

DRX behaviour is clearly seen in strain rates 1 and 10 at 1100°C but at high strain rate 20 and 1100°C, due to the dynamic strain ageing and strain hardening behaviour, there has been no DRX.

Chapter 6

Conclusions

1. The partial precipitation of copper was observed in the aging temperature of 300°C for 30 minutes. This was also confirmed by small increase in the hardness value.
2. The precipitation of tungsten has occurred at high temperature of 850°C. This observation was also verified by SEM and hardness values. There has been a sudden increase in the hardness values.
3. The precipitation of various intermetallic phases was also observed in the following research work.
4. Gleeble thermo-mechanical simulator was used to perform hot compression test on alloyed 2205 DSS, which showed dynamic recrystallization behaviour(DRX) at strain rate 1, 10 and temperature 1100°C.
5. Hot compression at high strain of 20 showed dynamic strain ageing behaviour i.e. serrations in the stress-strain curve.
6. Other phenomena's like dynamic recovery (DRV), strain hardening, softening mechanism were also observed after hot compression testing at various strain rates and temperatures.

Chapter 7

Suggestions for Future Work

1. Transmission electron microscopy (TEM) can also be performed to predict the nature of precipitations that have occurred at various ageing temperatures.
2. Gleeble simulator testing at plain strain condition with low strain rates can also be performed for more proper results on dynamic recrystallization behaviour.
3. Metallography study after Gleeble can be done to confirm the dynamic recrystallization behaviour due o hot compression.

References

1. Introduction to physical metallurgy By Sidney H. Avner.
2. Heat treatment By T.V. Rajan, C. P. Sharma and Ashok Sharma.
3. J.-O. Nilsson, Super duplex stainless steel, 1992.
4. Duplex brochure, Jindal stainless steel limited, Hisar.
5. Prabhu Paulraj, Rajnish Garg, Effect of intermetallic phases on corrosion behaviour and mechanical properties of duplex stainless steel and super duplex stainless steel 27(2015) 87-105.
6. Duplex families and applications: A review Part 2: From 1991 to nowdays By Jacques Charles.
7. Charecterization of the GTAW fusion line phases for superferritic stainless steel weldments by Ahmed H ElSawy, Journal of metal processing technology Volume 118, issue-3 Dec 2001 page 127-131.
8. Soon Hyeok Jeon, Soon Tae Kim, In Sung Lee, Joo Hyun Park, Kwang Tae Kim, Effect of copper addition on the formation of inclusions and the resistance to pitting corrosion of high performance duplex stainless steels 53(2011) 1408-1416.
9. Duplex stainless steels by Robert N Gunn, Elsevier, 1997.
10. García García D.M., García Antón J., Igual Mu ñoz A., Blasco Tamarit E., Effect of cavitation on the corrosion behaviour of welded and non-welded duplex stainless steel in aqueous LiBr solutions. Corros. Sci. 2006, 48, 2380–2405.
11. Yang Y., Wang Z., Tan H., Hong J., Jiang Y., Jiang L, et al. Effect of a brief post-weld heat treatment on the microstructure evolution and pitting corrosion of laser beam welded UNS S31803 duplex stainless steel. Corros. Sci. 2012, 65, 472–480.
12. Pekkarinen J., Kujanpää V. The effects of laser welding parameters on the microstructure of ferritic and duplex stainless steels welds. Phys. 2010(5), 517–523.
13. Karlsson L. ,Intermetallic phase precipitation in duplex stainless steels and weld metals: Metallurgy, influence on properties, welding and testing aspects. 1999.
14. Sieurin H., Sandström R.. Sigma phase precipitation in duplex stainless steel 2205. Mater. Sci. Eng.A 2007, 444, 271–276.
15. Martins M., Casteletti L.C. Sigma phase morphol-ogies in cast and aged super duplex stainless steel. Mater. Charact. 2009, 60, 792–795.
16. Chen T.H, Yang J.R. Effects of solution treatment and continuous cooling on σ-phase precipitation in a 2205 duplex stainless steel. Mater. Sci. Eng. A 2001, 311, 28–41.
17. Hsieh C-C, Wu W. Overview of intermetallic sigma phase precipitation in stainless steels. ISRN metal. 2012, 1-16.
18. Escriba D.M, Materna-Morris E., Plaut R.L., Padilha A.F. Chi-phase precipitation in a duplex stainless steel. Mater Charact 2009;60:1214–1219.
19. Ramirez A.J., Lippold J.C., Brandi S.D. The relationship between chromium nitride and secondary austenite precipitation in duplex stainless steels. Metall. Mater. Trans. A 2003, 34A, 1575–1597.
20. Cui J., Park I., Kang C., Miyahara K. Degradation of impact toughness due to formation of r phase in high nitrogen 25Cr-7Ni-Mo duplex stainless steels. ISIJ Int. 2001, 41, 192–195.

21. Lo K.H., Shek C.H., Lai J.K.L. Recent developments in stainless steels. Mater. Sci. Eng. A 2009,65, 39–104.
22. Sahu J.K., Krupp U., Ghosh R.N., Christ H.-J. Effect of 475°C embrittlement on the mechanical properties of duplex stainless steel. Mater. Sci.Eng. A, 2009, 508, 1–14.
23. Duplex families and applications: A review Part 3: From 1991 to nowdays By Jacques Charles.
24. Soon-Hyeok Jeon, Soon-Tae Kim, In Sung Lee, Effects of Cu on the precipitation of intermetallic compounds and the intergranular corrosion of hyper duplex stainless steels, Corrosion science 66 (2013) 217-224.
25. Soon-Hyeok Jeon, Soon-Tae Kim, In Sung Lee, Effect of copper addition on the formation of inclusions and the resistance to pitting corrosion of high performance duplex stainless steels, Corrosion science 53 (2011) 1408-1416.
26. Quigxuan Ran, Jun Li, Yulai Xu, Xueshan Xiao, Haifeng Yu, Novel Cu-bearing economical 21Cr duplex stainless steel, Materials and design 46 (2013) 758-765.
27. K. Ogawa, H. okamoto, M. Igarashi, M. Ueda, T.Mori, T. Kobayashi, Weld Int. 11 (1997) 14-22.
28. J. S. Kim, H. S. Kwon, Corrosion 55 (1999) 512-521.
29. C.J. Park, M. K. Ahn, H.S. Kwon, Material Science and Engineering A 418 (2006) 211-217.
30. Freire E. Differential scanning calorimetry. Methods Mol Biol. 1995; 40: 191-218.
31. Masayuki Sagara, Yasuyuki Katada, and Toshiaki Kodama, 2003, Localized Corrosion Behavior of High Nitrogen-bearing Austenitic Stainless Steels in Seawater Environment, ISIJ International, Vol. 43 (2003), No. 5, page. 714–719.
32. Y. Katada, N. Washizu, and H. Baba, 2005, Development of High-Nitrogen Steels in The National Institute For Materials Science, Metal Science and Heat Treatment Vol. 47, Nos. 11 – 12, 2005.